NASA Contract NAS8-31359

FINAL REPORT

DEVELOPMENT OF A MICROBALANCE SUITABLE FOR SPACE APPLICATION

Prepared for

George C. Marshall Space Flight Center

By:

Harvey Patashnick
Research Associate
Dudley Observatory
Plaza 7, 1202 Troy-Schenectady Rd.
Latham, New York 12110

Georg Rupprecht
Consultant
7150 E. Berry Avenue
Englewood, Colorado 80110

Approved by:

Curtis L. Hemenway
Director,
Dudley Observatory

24 June 1977

FOREWORD

This report was prepared by Dudley Observatory under contract NAS8-31359, "Development of a Microbalance Suitable for Space Application", for the George C. Marshall Space Flight Center of the National Aeronautics and Space Administration under the technical cognizance of Dr. Nicholas C. Costes of the Space Sciences Laboratory of MSFC.

CONTENTS

CONTENTS (continued)

1. INTRODUCTION

The Tapered Element Oscillating Microbalance (TEOM)* is a new ultra-sensitive mass measurement device which is suitable for both particulate and vapor deposition measurements. It has many advantages over other micro-weighing devices and should be of interest to anyone involved in contamination measurements, surface reaction studies, particulate monitoring systems or any micro-weighing activity where either laboratory or field monitoring capability is desired.

The TEOM is significantly different from other types of gravimetric or quartz crystal microbalances (QCM's). The active element of the TEOM consists of a tube or reed constructed of a material with high mechanical quality factor and having a special taper. The element is firmly mounted at the wide end while the other end supports a substrate surface which can be composed of virtually any material. The tapered element with the substrate at the free (narrow) end is set into oscillation in a clamped-free mode. A feedback system maintains the oscillation whose natural frequency will change in relation to the mass deposited on the substrate. The mass sensitivity and frequency of a particular unit can be chosen at will by proper dimensioning of the oscillating tapered element. Unlike most other microbalances, the TEOM can be made inexpensively, is mechanically strong and is easily fully automated. The output consists of frequency

* The TEOM is a proprietary device.

information in the 10 to 10^3 Hz region. A photograph of a typical instrument is shown in Figure 1. With the unit illustrated here masses from a single monolayer to milligrams can be weighed with one to 10 sec. time resolution.

In order to demonstrate the advantages of the TEOM for real-time particulate monitoring, for example, a comparison with a QCM is useful since QCM's are currently used for particulate detectors in commercially available instrumentation.

QCM's, as they were used originally, have typically been restricted to the measurement of uniformly deposied thin films. The necessity for a uniform layer deposition is due to the variation of mass sensitivity across the QCM surface, and the requirement for a thin film is dictated by the need for sufficiently strong adhesive forces so that no displacement occurs between the QCM surface and the deposited sample as a consequence of the high surface acceleration of the device. Thick layers lead to saturation effects. In order to monitor deposition of particulate material, an oil coating is needed on the crystal surface to bond the particulates. Since the QCM is not uniformly sensitive to mass across its surface, a narrow impaction jet is used to deposit particles at a particular location and thus allow a meaningful measurement. The utilization of a small impact site results in site saturation effects when the particle density becomes too high to have additional material bond properly.

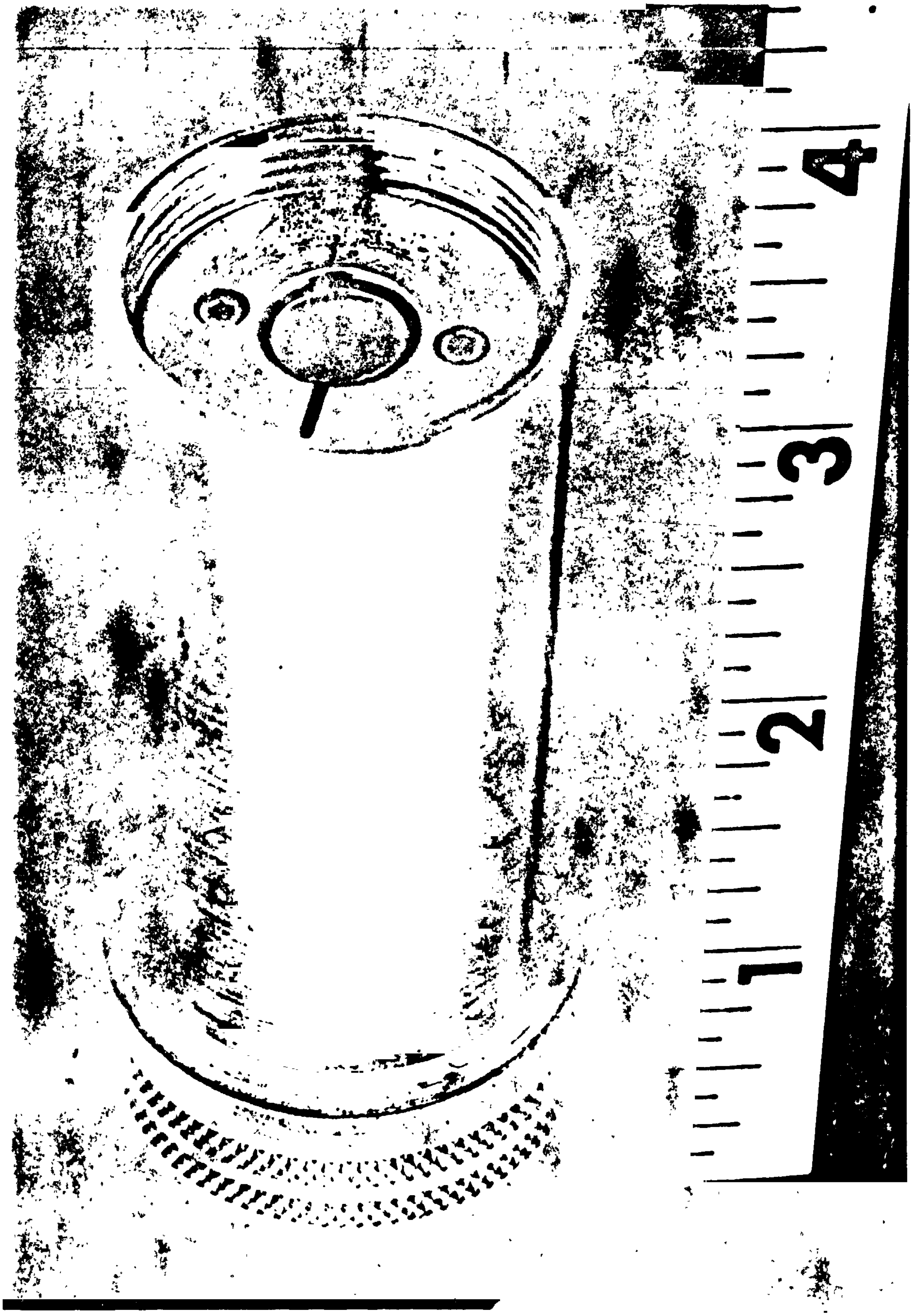

FIGURE I

The TEOM, on the other hand, is inherently very suitable for particulate measurements since its surface acceleration is orders of magnitude below that of a QCM, and it is uniformly sensitive to mass across the entire substrate surface. This eliminates the need for a narrow impaction jet allowing a relatively large surface area available for particle capture which, along with a low surface acceleration, drastically reduces saturation effects and enables the measurement of larger particulate masses. Furthermore, virtually any type of substrate can be used (filters, oil coated surfaces, reactive surfaces, etc.). The substrate can also be removed and taken for laboratory analysis. The collected particles could then be investigated by scanning electron microscopy for particle sizes and shapes and by x-ray energy dispersive analysis for elemental composition.

The TEOM, although highly sensitive, has a sufficiently large dynamic range due to its low susceptibility to saturation, to allow unattended sampling for long periods of time. It can be used as a dust fall monitor or it could be as a detector in an impactor. A network of such monitors tied to a central monitoring and control station, for example, could enable real-time mass concentration measurements of airborne particulates over an extended area with a minimal manpower requirement.

In the first field application of the TEOM, it was used as the detector in a micrometeorite collection experiment flown on a high altitude balloon. The instrument was placed at the bottom of a 24' diameter funnel and launched to an altitude of 80,000 feet. A photograph of the device in place under the funnel is shown in Figure 2. The data was telemetered to a ground station during the flight and recorded on a real-time basis. At the termination of the flight, the unit was ejected and parachuted down from the balloon altitude. It was recovered without damage along with the collected particles which are now available for laboratory analysis. A portion of the results from this flight is shown in Figure 3.

There are many applications for this new device which range from real-time monitoring of particulate concentration in the ambient air to vacuum deposition measurements and thermogravimetric analysis. Instruments delivered under this contract are being evaluated by Marshall Space Flight Center for use as a contamination monitor on board the Space Shuttle.

1.1 Essential Features of the TECM - The first model of a TEOM was delivered to MSFC at the end of October 1975. Figure 4 shows the essential components of the device and a block diagram of the electronic feedback system. Also shown is a thermistor which in the first model was placed within several millimeters of the oscillating tapered element to monitor the ambient temperature within the cylindrical envelope of the device.

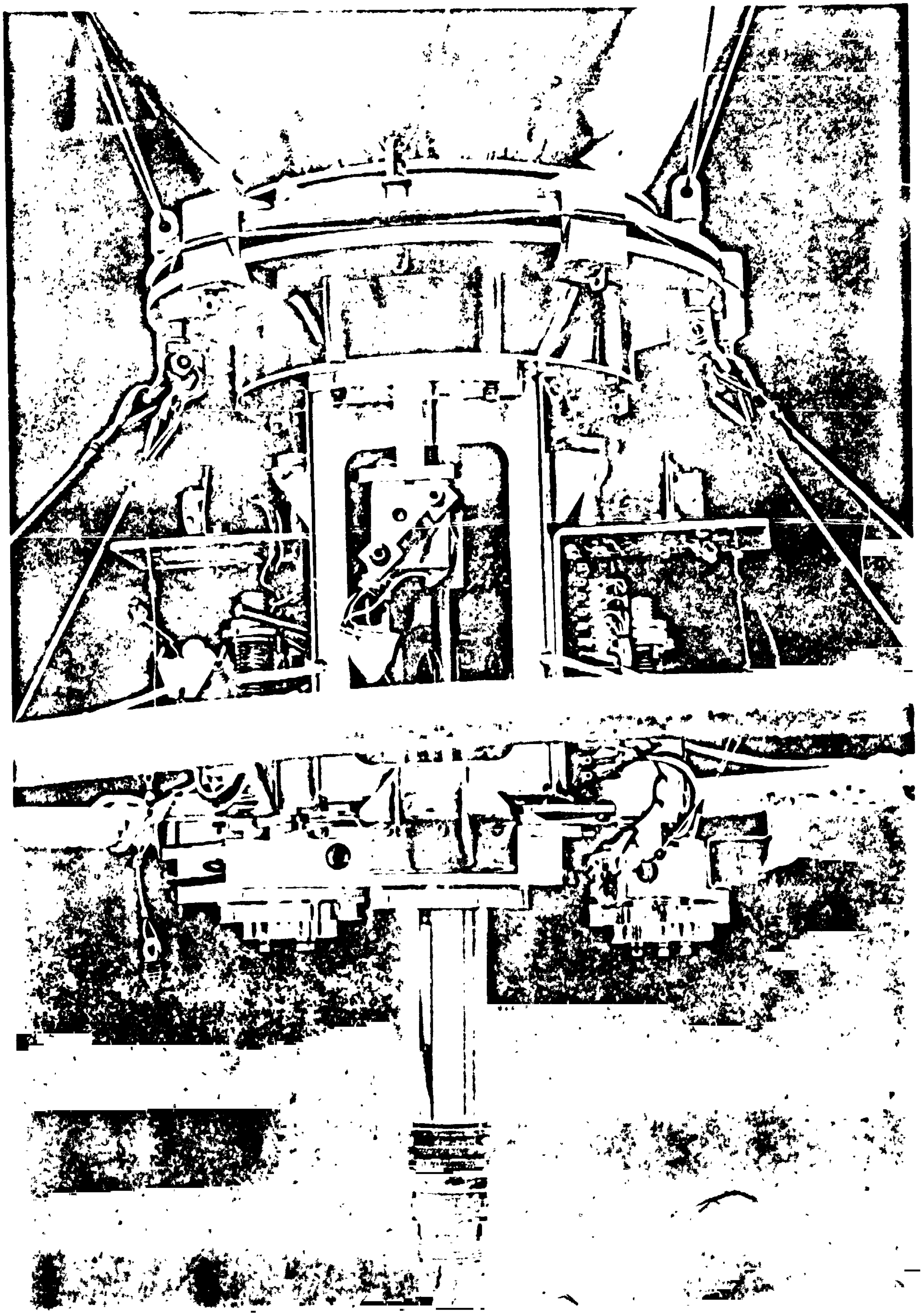

FIGURE 2

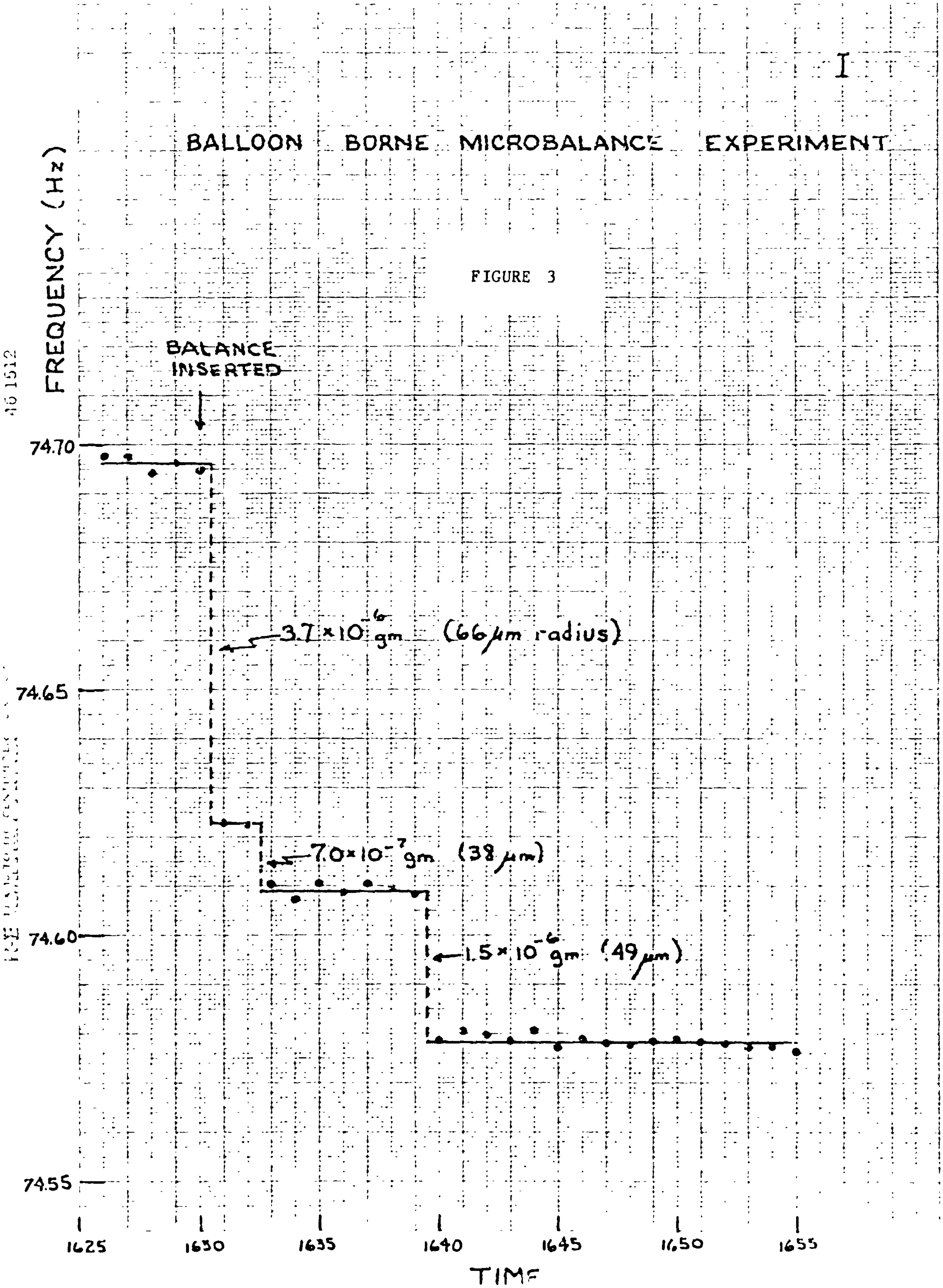
I
BALLOON BORNE MICROBALANCE EXPERIMENT
FIGURE 3
FREQUENCY (Hz)
BALANCE INSERTED
74.70
74.65
74.60
74.55
3.7×10⁻⁶ gm (66 μm radius)
7.0×10⁻⁷ gm (38 μm)
1.5×10⁻⁶ gm (49 μm)
1625
1630
1635
1640
1645
1650
1655
TIME

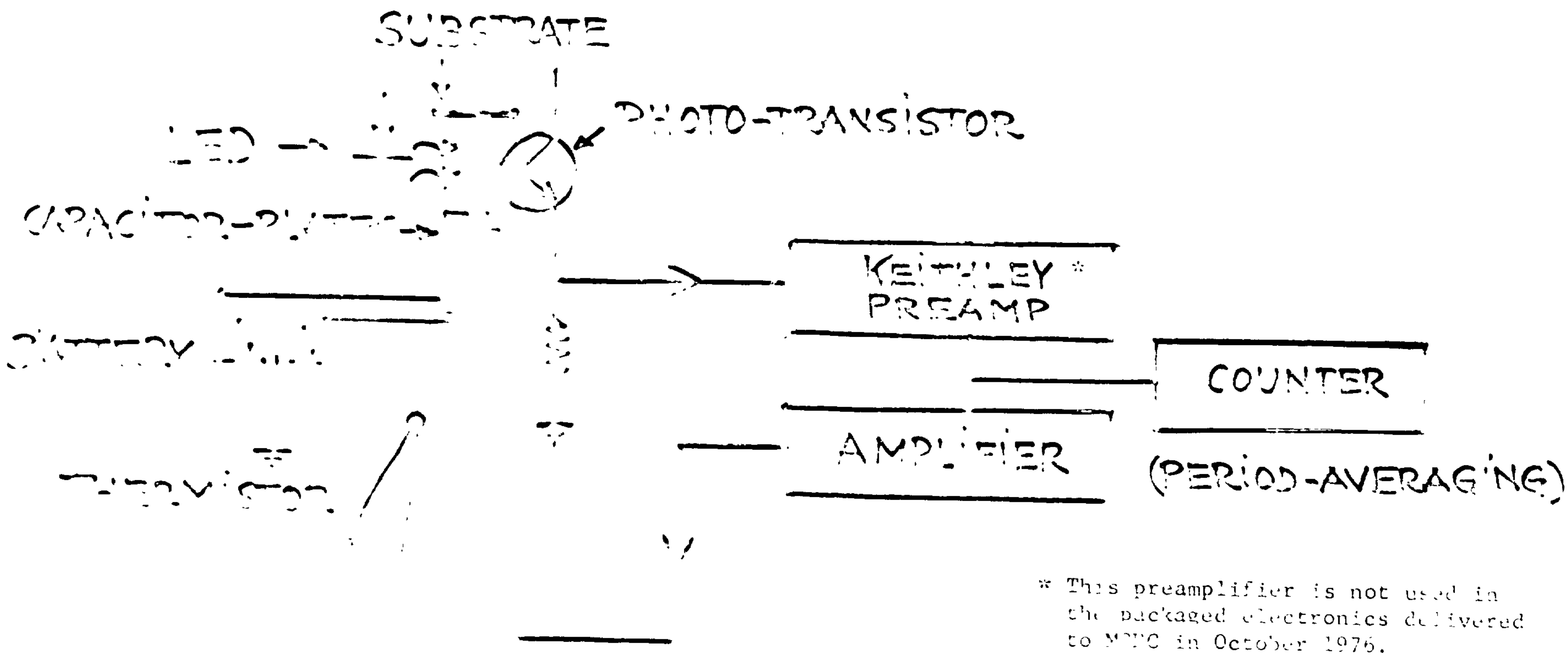

* This preamplifier is not used in the packaged electronics delivered to MTC in October 1976.

[illegible] - [illegible] SYSTEM

1.2 Experimental Experiences - This first device clearly demonstrated the feasibility and potential of the instrument. The sensitivity of the device was determined to be approximately 5×10^{-5}g/Hz. Since the frequency resolution was in the order of 0.001 Hz the mass resolution capability was 5×10^{-8}g. Measurements with single particulate masses demonstrated accurate and reproducible results.

Extended testing of the device, however, revealed a number of apparent problems. These can be described as follows:

1. Frequency instabilities - These included short term fluctuations of the order of a few millihertz and long term drifts of varying magnitude and unpredictable nature.

2. Frequency dependence on amplitude - Although this is expected for any oscillator with anharmonic potential terms, it is desirable to reduce this effect to obtain the highest mass resolution possible.

3. Frequency shifts with variation of the harmonic content of the driving voltage in the feedback system - When the preamplifier bandpass was changed, the frequency of the device at constant mass loading would shift. Also, the fiber would tend to change amplitude and reach a stable oscillation only when the driving waveform had a high harmonic content.

4. Lack of frequency and temperature correspondence during temperature changes - The frequency of the device at constant mass

loading did not track properly with the temperature reading of the thermistor during temperature transients. This made mass measurements under any but equilibrium conditions inaccurate.

5. Mechanical Shortcomings - In working with the device, fiber adjustment and removal proved to be inconvenient and cumbersome.

There are basically two approaches to deal with these problems. One approach is to avoid these difficulties by many calibration procedures, or one can work toward an understanding of the reasons for these problems and try to correct them in a more fundamental way. By taking the second approach, it was felt that the instrument could be reduced to its simplest and most stable mode of operation.

It was noticed that all the changes which were introduced during experimentation were coupled with amplitude changes. In order to separate the interrelated effects, it became apparent that the introduction of an amplitude control system was a necessary step.

2. AMPLITUDE CONTROL STUDY

2.1 Development of a Detector for the Mechanical Amplitude of the Fiber - In Figure 5, the frequency dependence on amplitude is shown for a typical device. As an indication of fiber amplitude, the preamplifier (Keithley 103A) output which is an indication of the phototransistor output is used. From the frequency dependence on the amplitude shown in the figur , one can extract the expression $\frac{\Delta f}{f} \Big/ \frac{\Delta A}{A} = 10^{-3}$.

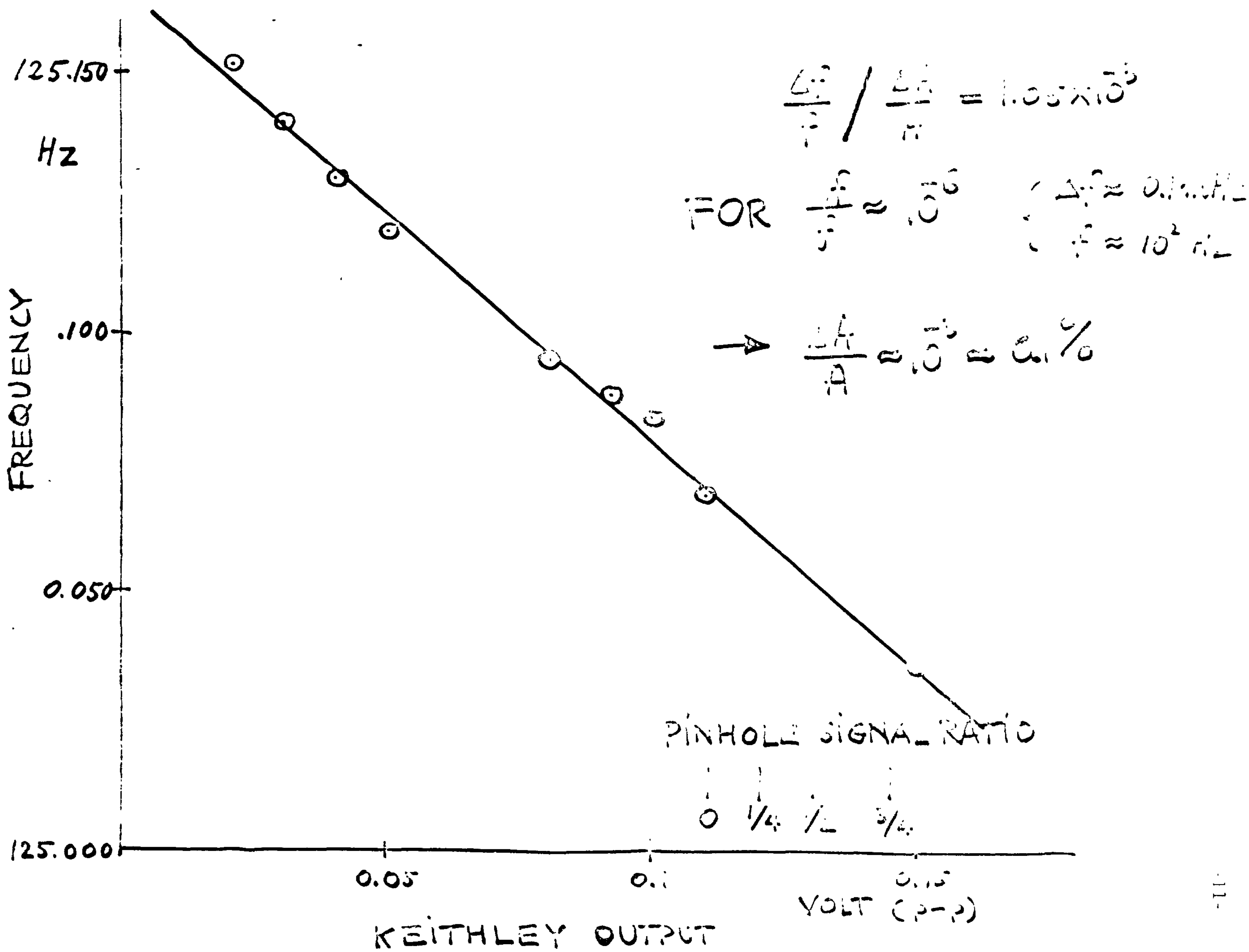

FREQUENCY DEPENDENCE ON AMPLITUDE
Figure 5

If one wishes to maintain a frequency resolution of 10^{-4} Hz, one finds at a frequency of about 100 Hz for the value of $\frac{\Delta f}{f} \approx 10^{-6}$. This implies that for this frequency resolution the amplitude must be controlled to $\frac{\Delta A}{A} \approx 10^{-3}$ or 0.1%. The indication of the pinhole signal in Figure 5 will be explained shortly.

The control of the amplitude to within 0.1% requires a sustantial effort. It should be emphasized that the goal is not to maintain the output of the phototransistor constant, but to keep the mechanical amplitude of the fiber under control. The reason is that the output of the phototransistor may vary (due to temperature changes for example) as well as the outputs of the photodiode and the amplifier. However if a means could be devised to keep the mechanical amplitude constant, than the variations in the electrical components are bypassed.

In Figure 6, the principle of the mechanical amplitude detector is explained. The section of the figure labeled (A) shows the functional arrangement of the essential parts of the amplitude detector. The radiation from a photodiode backlights the vibrating fiber. A lens projects the shadowed image of the fiber onto an opaque screen in which contains a pinhole of approximately 100 μm diameter. The light which enters the pinhole is registered by a phototransistor behind the pinhole. The pinhole is offset from the rest position of the fiber. When the image of the fiber oscillates with an amplitude commensurate with the offset of the pinhole as shown in (B), the light through the pinhole is

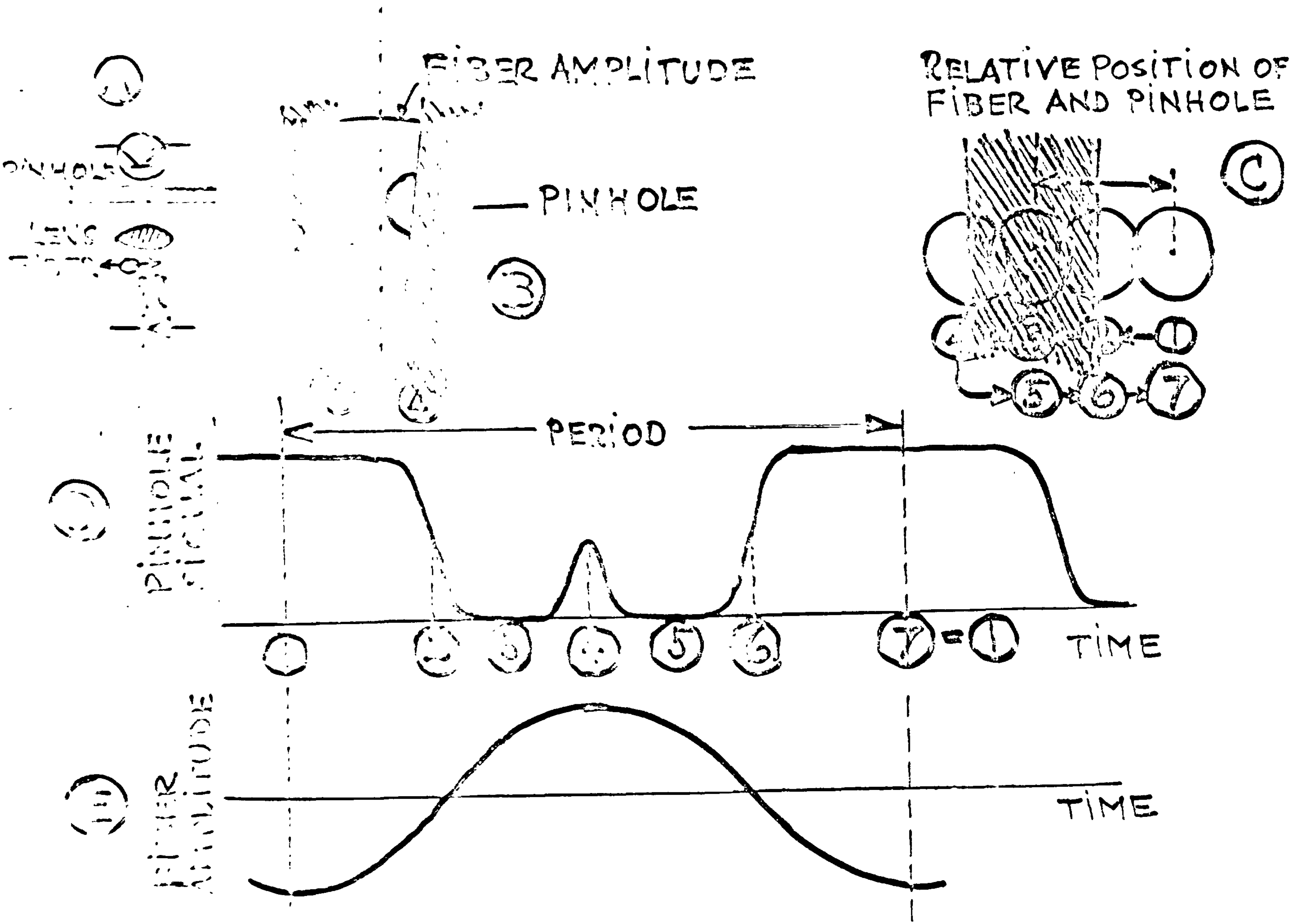

AMPLITUDE DETECTOR
Figure 6

modulated as indicated in (D). This corresponds to the fiber oscillation shown in (E). In (B), the motion of the fiber image is shown in its extreme maximum amplitude positions indicated by (1) and (4). Since the pinhole signal depends only on the relative position of pinhole and fiber image, a representation utilizing a fixed fiber reference as shown in (C) is useful. The different positions (1) - (7) are indicated, and the corresponding pinhole signals are shown in (D). Attention should be drawn to the signal at (4) whose amplitude is dependent upon how much of the pinhole is uncovered during the positive maximum of the fiber oscillation. Since the lens amplifies the fiber diameter, the signal at (4) is a very sensitive indication of the maximum fiber position and thus of its amplitude. The absolute value of the signal at (4) is also dependent on the output of the photo-electronics and proceeding gain stages. However, the ratio of the signal at (4) is solely dependent on the mechanical amplitude of the fiber and is not influenced by variations of electronic components. This is the pinhole signal ratio referred to in Figure 5. A series of oscillographs demonstrating the effect of different fiber amplitudes on the pinhole signal is shown in Figure 7.

The utilization of this detection system for the mechanical amplitude in an amplitude control system is explained next.

2.2 Amplitude Control System Electronics

2.2.1 System Layout - The basis underlying this control technique

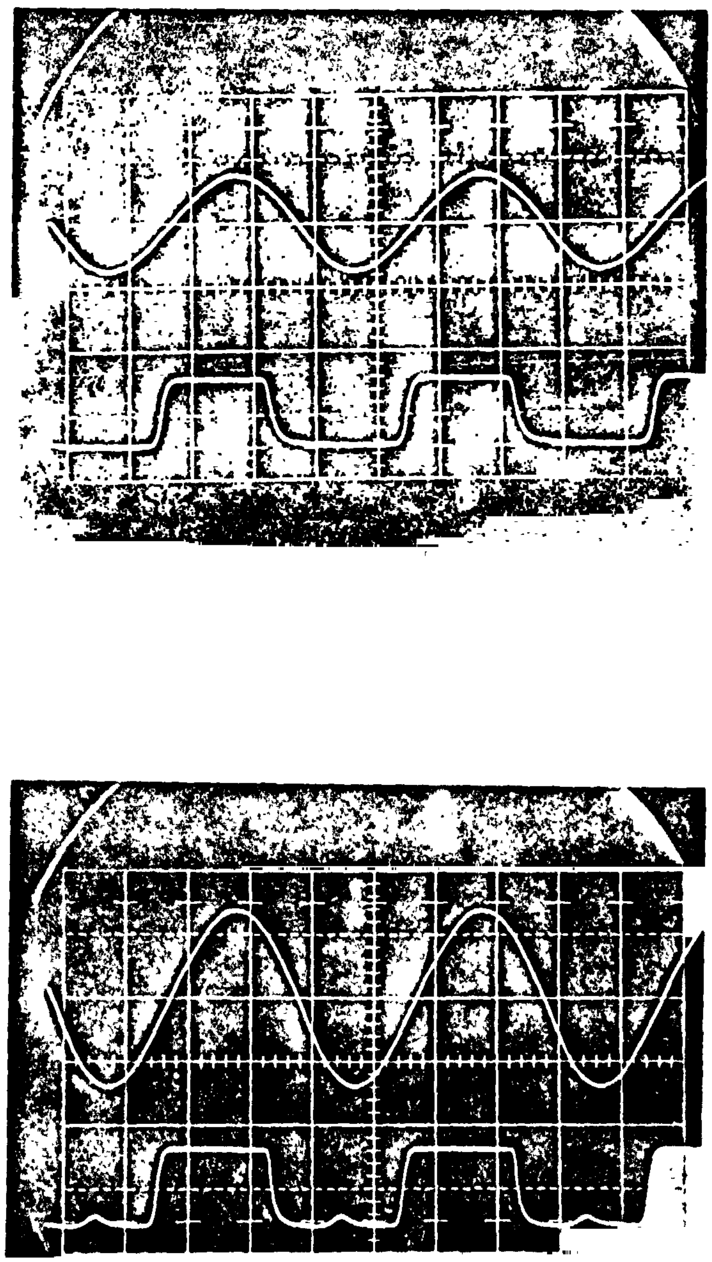

KEITHLEY OUTPUT
0.05 v/cm

PINHOLE SIGNAL
0.005 v/cm

FIBER AMPLITUDE AND PINHOLE SIGNAL

Figure 7

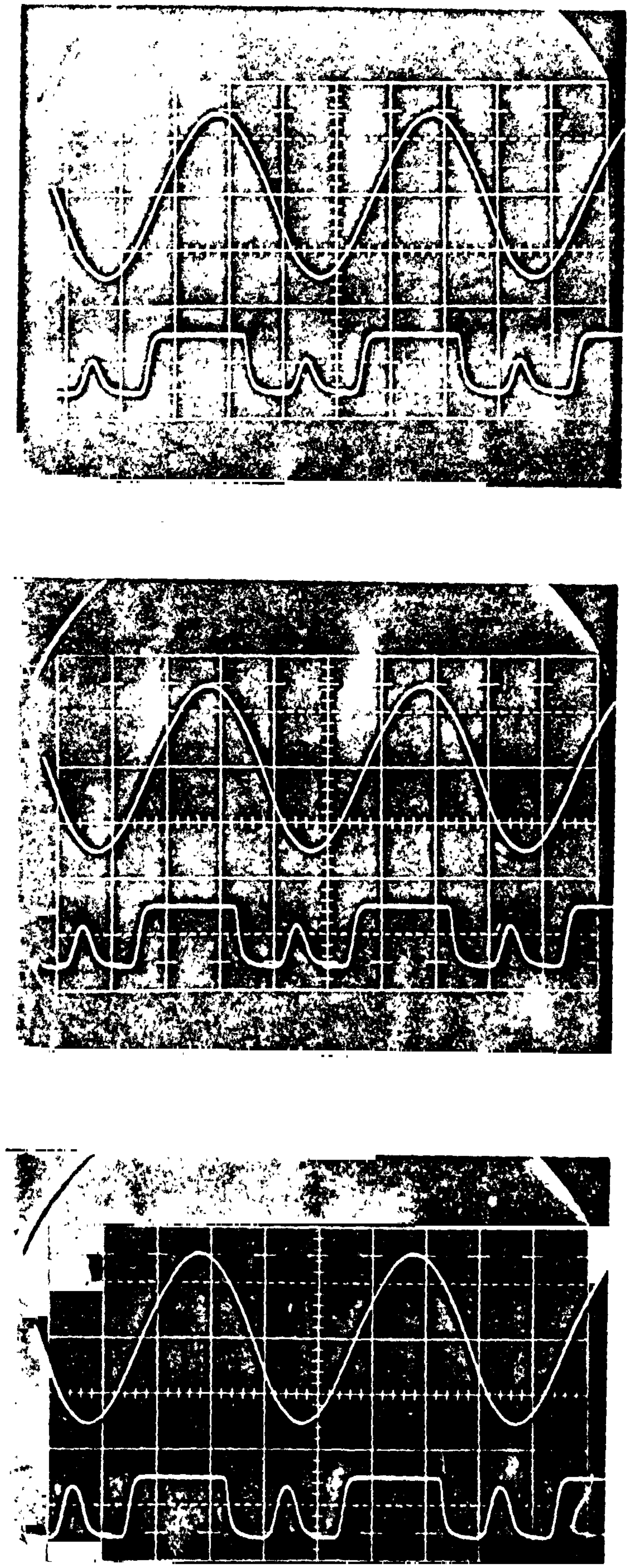

Figure 7 (continued)

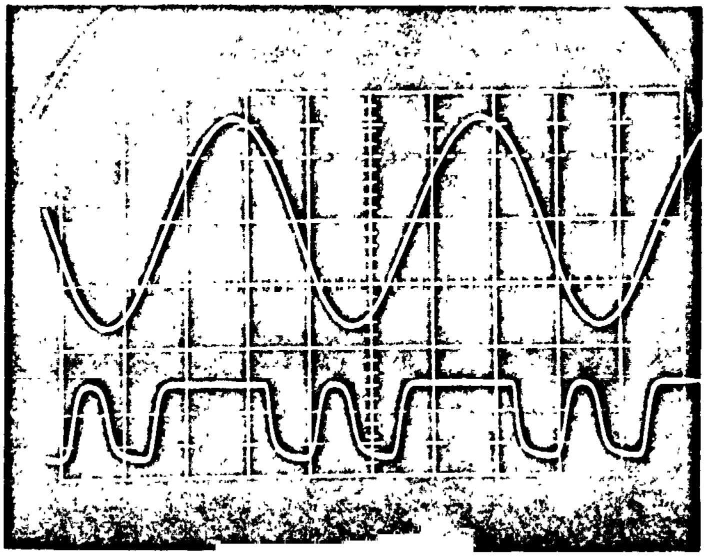

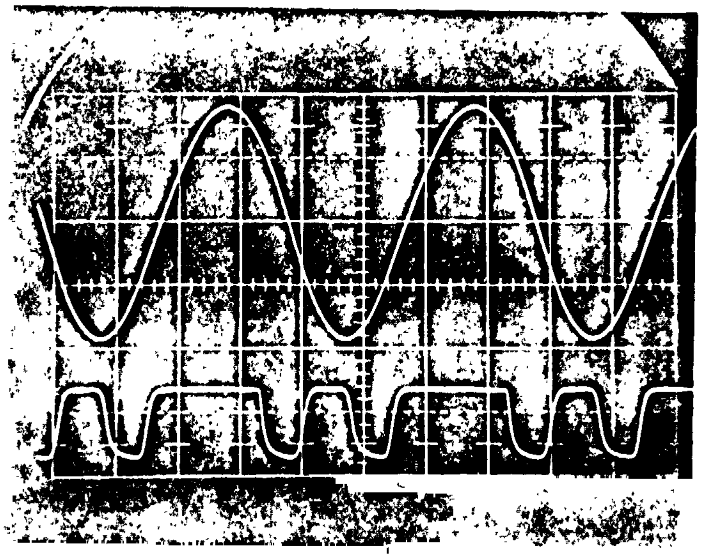

Figure 7 (Continued)

is that the amplitude of the pinhole secondary pulse is functionally related to the mechanical amplitude of the vibrating fiber and that information derived from this signal can be used to control the drive level to the fiber and thereby control its amplitude.

As seen from Figure 7, the pinhole signal is composed of a large flat-topped portion and a small secondary pulse. The saturated pinhole signal is very nearly in phase with the positive-going half of the main signal; the secondary pinhole pulse nearly coincides with the negative-going portion of the main signal; and these phase relationships are independent of signal amplitude.

The overall electronic system based on the pinhole technique described above is shown in block diagram form in Figure 8. For a first look it is convenient to subdivide the diagram into a few sections. The top row represents the main signal path used to actually drive the fiber. This is the signal to be controlled by the rest of the system. The pinhole signal is processed by the next two rows in the diagram. From this signal an error signal is derived and used to correct the main signal amplitude. The bottom row of the diagram represents "housekeeping" functions of the control system derived from the main and pinhole signals and the actual control function generator.

2.2.2 System Description - The main signal, in addition to being used to drive the fiber through a feedback loop is processed to provide timing for the control functions. The amplified main signal is converted

FOLDOUT FRAME

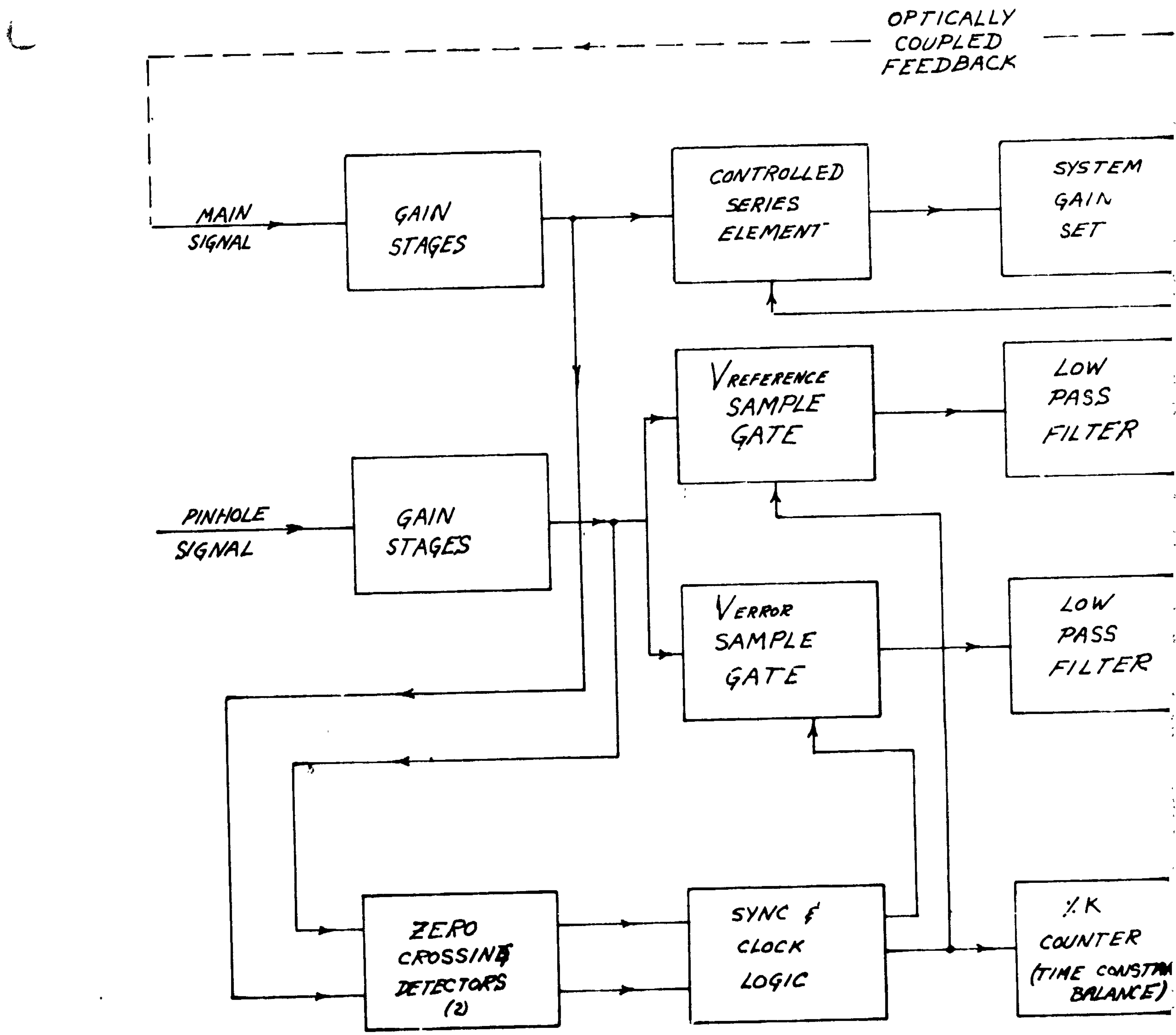

FOLDOUT FRAME

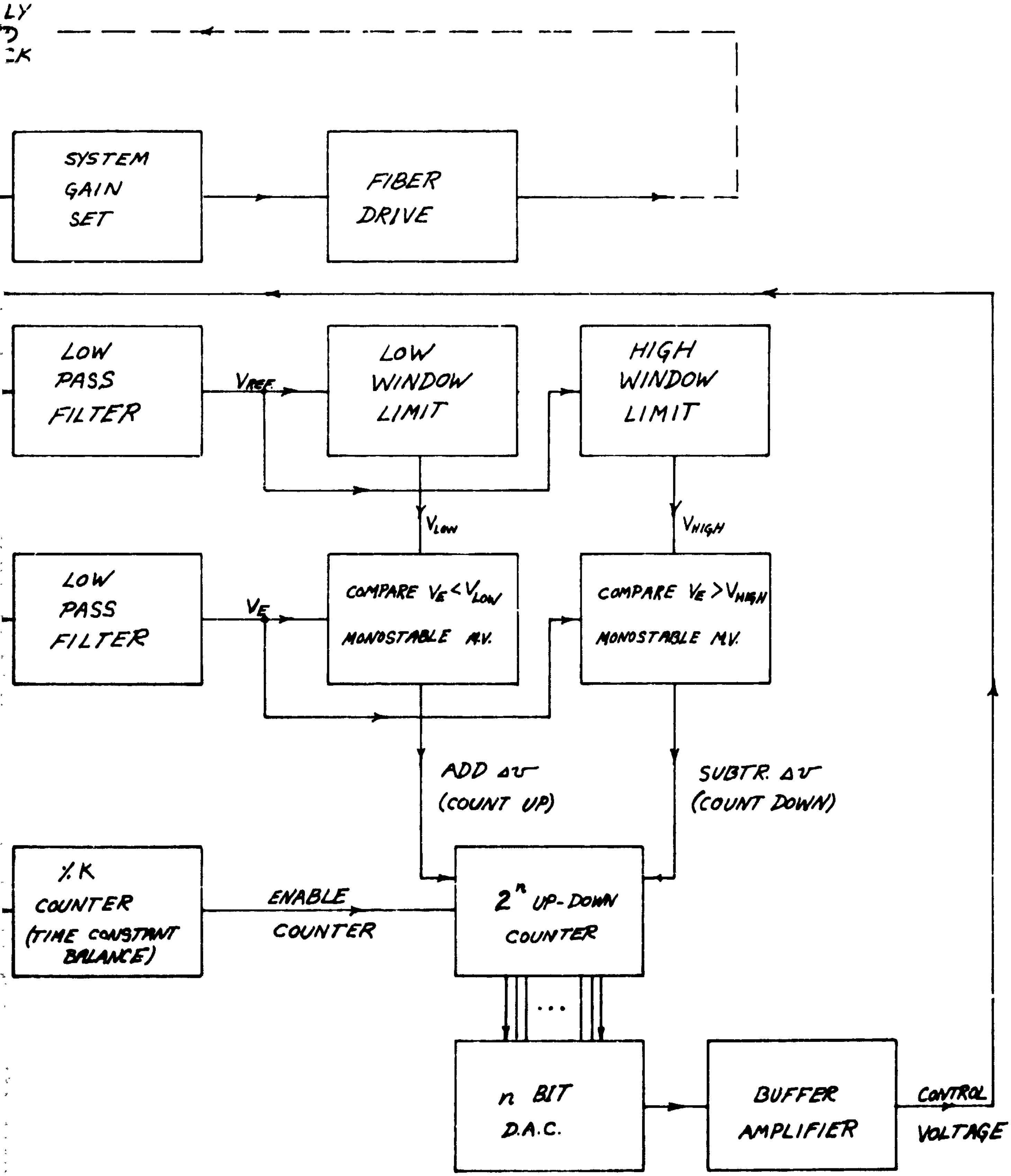

Figure 8

to logic compatible switching functions by means of a zero-crossing detector. This detector is simply a high speed comparator using a ground reference as one input. The comparator output switches instantaneously (< 1 μsec) between the 0v and +5v stable states depending upon whether the signal input is less than or greater than the reference input. Compared to the main signal period of $\sim$10 msec. the switching delays are completely negligible.

The pinhole detection scheme is most sensitive when the secondary pinhole signal was about half the amplitude of the flat-topped pinhole signal. The control portion of the system was therefore designed to maintain the pulse amplitude between two arbitrarily close preset voltages near the point where the ratio of the secondardy pulse amplitude to the flat-topped amplitude was one half.

The secondary pinhole pulse contains the information necessary to control the fiber amplitude, it is therefore necessary to separate the secondary pulse from the saturated signal. This is accomplished by using a gate pulse derived from the negative portion of the main signal. A field effect transistor in series with the pinhole signal amplifier output is turned on and off by this gating pulse so as to allow only sampling of the secondary pinhole signal. In order to mininize fluctuations due to possible stray noise pulses in the system, the output from the FET series switch is applied to a low pass RC filter to provide a filtered DC output signal representative of the average value of the pinhole pulse signal.

A second FET series gate, timed to coincide with the flat-topped pinhole signal and followed by filtering and gain conditioning was used to generate the reference voltage for the system (V reference on block diagram). Comparators are then used to detect the "less than minimum" and "greater than maximum" error conditions with the no error condition fulfilled when the secondary pulse amplitude was approximately half the flat-topped pinhole signal amplitude.

Both comparator outputs are gated and fed to the inputs of monostable multivibrators (compare blocks in the diagram). When either comparator output is high during gate time (they cannot both be high simultaneously), the corresponding multivibrator transmits one and only one pulse to an input of an up-down counter. The counter in turn is used to set the output of a DAC (digital to analog converter) which generates the actual control voltage used to control the drive level to the fiber.

A further consideration for the control system is that the time constant of the control voltage generator (the DAC) be at least approximately matched to the mechanical time constant of the vibrating fiber. Measurements of the fiber time constant indicated a time of several seconds in response to a small (1%) change in drive level. The pinhole signal amplitude, on the other hand, is gated once during each fiber period, or at a rate of about 100 Hz; therefore the up-down counter controlling the DAC would be overdriven by a direct input from the comparator one shots. The result of this overdrive would be that the system would be continually "hunting" a stable amplitude condition. This difficulty was eliminated by a divide by N counter which allows incrementing the DAC output comparable to the fiber time constant.

2.3 <u>Experience with the Amplitude Control System</u> - With a bench version of the amplitude control system installed, it was expected that a highly stable frequency would result. We found however that frequency jumps in the order of 10 millihertz occurred in a completely unpredictable fashion unrelated to any deliberate parameter change. Since these instabilities were introduced by the incorporation of the amplitude control system, and since the amplitude control system is linked in a critical way solely through the relative position between the pinhole and the fiber, it was concluded that a mechanical instability was causing the undersirable effect. If the fiber shifts with respect to the pinhole, the control system will readjust the amplitude to a new value to satisfy the preset signal ratio. This results in a frequency shift.

The source of the mechanical instability was found in the mounting of the fiber and the support structure on what originally appeared to be a sufficiently solid connector insert as illustrated in Figure 9a. In reality the support arms could move very slightly with respect to the fiber. In order to fix the relative position between fiber and the support structure and to improve the mechanical stability of the design, a fiber support platform as illustrated in Figure 9b was introduced. This

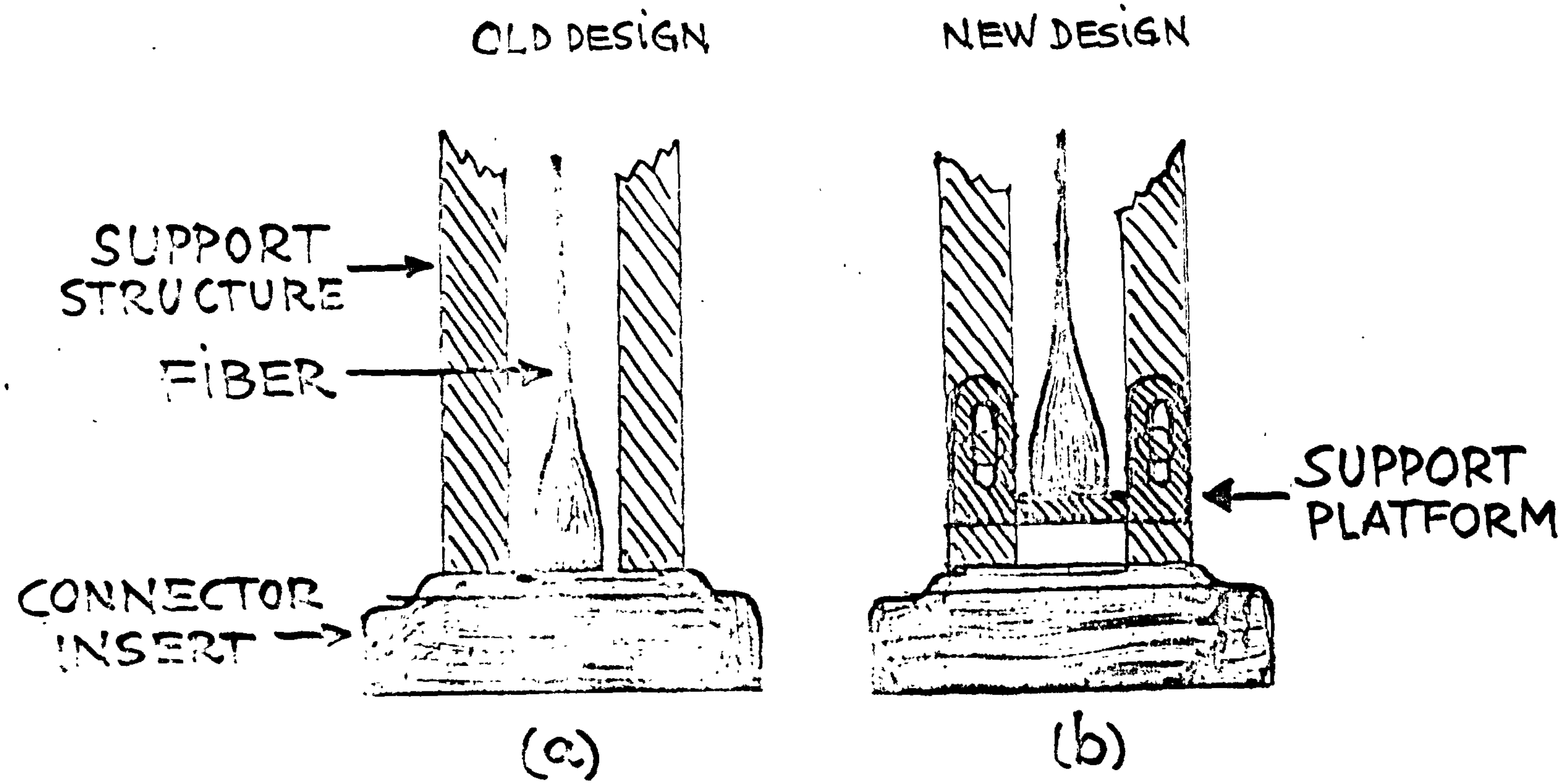

MECHANICAL STABILIZATION

Figure 9

alleviated the problem and served an additional benefit by making the adjustment and removal of the fiber much more convenient.

The next problem which was addressed concerned the influence of bandpass settings in the feedback system to the frequency. Since there was a dependence on the bandpass, the fiber oscillation was apparently influenced by higher harmonics in the drive signal. The obvious thing to do was to eliminate the harmonics by narrowing the bandpass of the amplifier. It was observed that the gain of the amplifier which was now controlled by the amplitude control system was rapidly increasing with decreasing bandwidth until finally there was not sufficient gain in the system to sustain the oscillation of the fiber. This clearly indicated that the fiber was not being driven by the fundamental excitation frequency. This pointed out that the feedback system was not providing an appropriate phase relation for the fundamental to drive the fiber. For this reason an amplifier was constructed which included a turnable filter with the effect that at the resonant frequency, fo, of the filter a phase shift of 90° would result. For $f > fo$, a phase shift greater than $\pi/2$ would occur while for $f < fo$, the phase shift was smaller than $\pi/2$. After this was accomplished, it was discovered that the frequency dependence on amplitude was a function of the phase shift. Some results are shown in Figure 10.

There are a number of advantages in providing a 90° drive to the

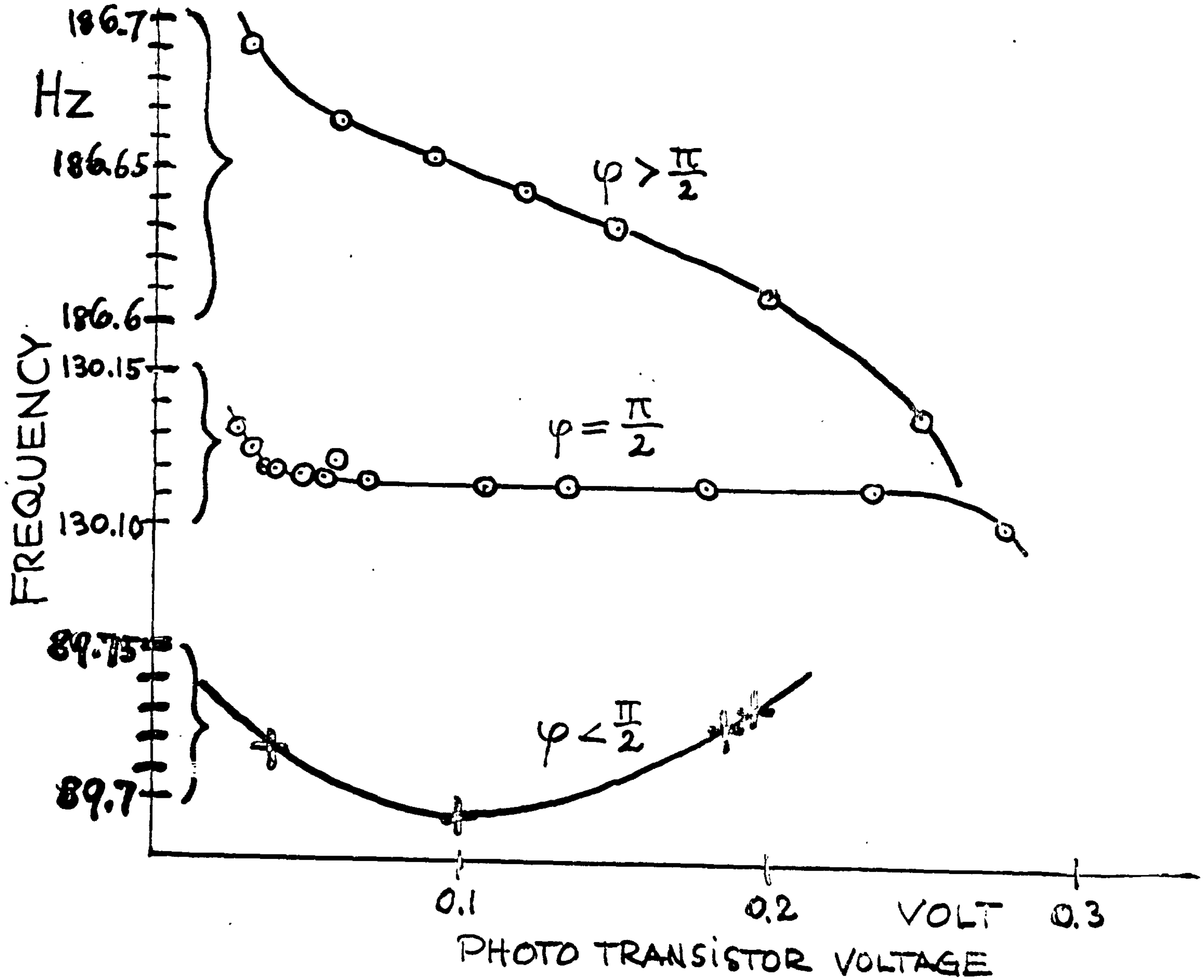

FREQUENCY AS A FUNCTION OF AMPLITUDE FOR DIFFERENT PHASE SHIFTS

Figure 10

fiber. As is apparent from the results shown in Figure 10, the frequency dependence on amplitude is drastically reduced so that the stringent requirements for an amplitude control system can be relaxed.

Aside from this benefit, the driving of the fiber with the fundamental frequency at 90° results in the fiber oscillating at its natural resonant frequency without being "pulled". This is evident by mechanically pulsing the fiber and measuring its frequency as its oscillation decayed without a feedback system and comparing this to the frequency under steady-state conditions with feedback.

Furthermore the energy transfer is most efficient with the $\pi/2$ - shifted drive resulting in the reduction of the driving potential both on the peak to peak voltage delivered by the amplifier to the fiber and a reduction of the dc electric field on the capacitor plates. The reduction of the plate voltage which was originally $\pm$ 300 vdc was reduced to $\pm$ 100 vdc.

3. THE INFLUENCE OF GRAVITY ON THE FIBER FREQUENCY

Experimentally it was noticed that the frequency of the fiber depended upon the orientation of the device with respect to local vertical. This can be understood by considering the potential energy storage of the device during vibration. In Figure 11, the fiber is illustrated oscillating in an upright and inverted situation. The potential well that determines the resonant frequency of the fiber is the total potential consisting of the elastic potential of the fiber and the gravitational

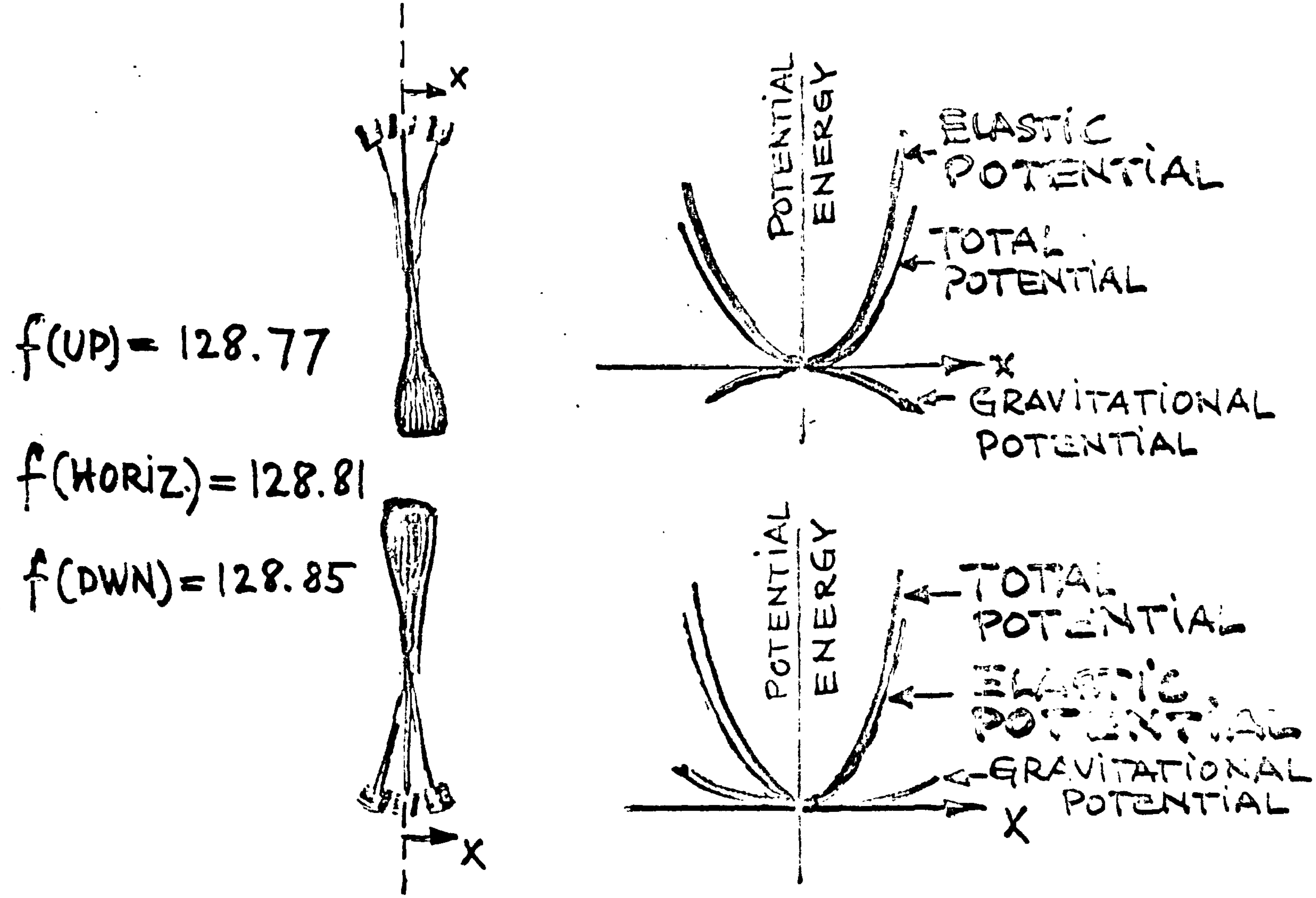

INFLUENCE OF GRAVITY ON THE
FIBER FREQUENCY

Figure 11

potential of the effective mass of the oscillating element. In an upright position the total potential has a smaller curvature than the elastic potential and hence the lowest frequency results when the device is upright. On the other hand, the total potential has a larger curvature than the elastic potential in the inverted position resulting in the highest frequency of any orientation. In the horizontal position the gravitational potential is ineffective to a first order resulting in a frequency which is representative of the elastic potential alone and which also would be expected under zero gravity conditions.

Consequently, in terrestrial application, one should take care of the fiber orientation or simply leave the orientation unchanged between measurements.

4. THE TEMPERATURE DEPENDENCE OF THE FREQUENCY

4.1 Steady-State Condition - When the oscillating element undergoes a temperature change, a change in frequency results. The relation between temperature and frequency is linear as can be seen in the data shown in Figure 12. Although df/dT depends upon loading for a given fiber, the quantity 1/f df/dT is a constant. For vycor fibers, we have found that the temperature sensitivity of the device can be represented by $1/f\ df/dT \approx 9 \times 10^{-5}\ (^{o}C)^{-1}$. Therefore when the device undergoes a temperature change, the frequency can be normalized to a base temperature by the expression:

$$f = 9 \times 10^{-5} \cdot f \cdot \Delta T \ .$$

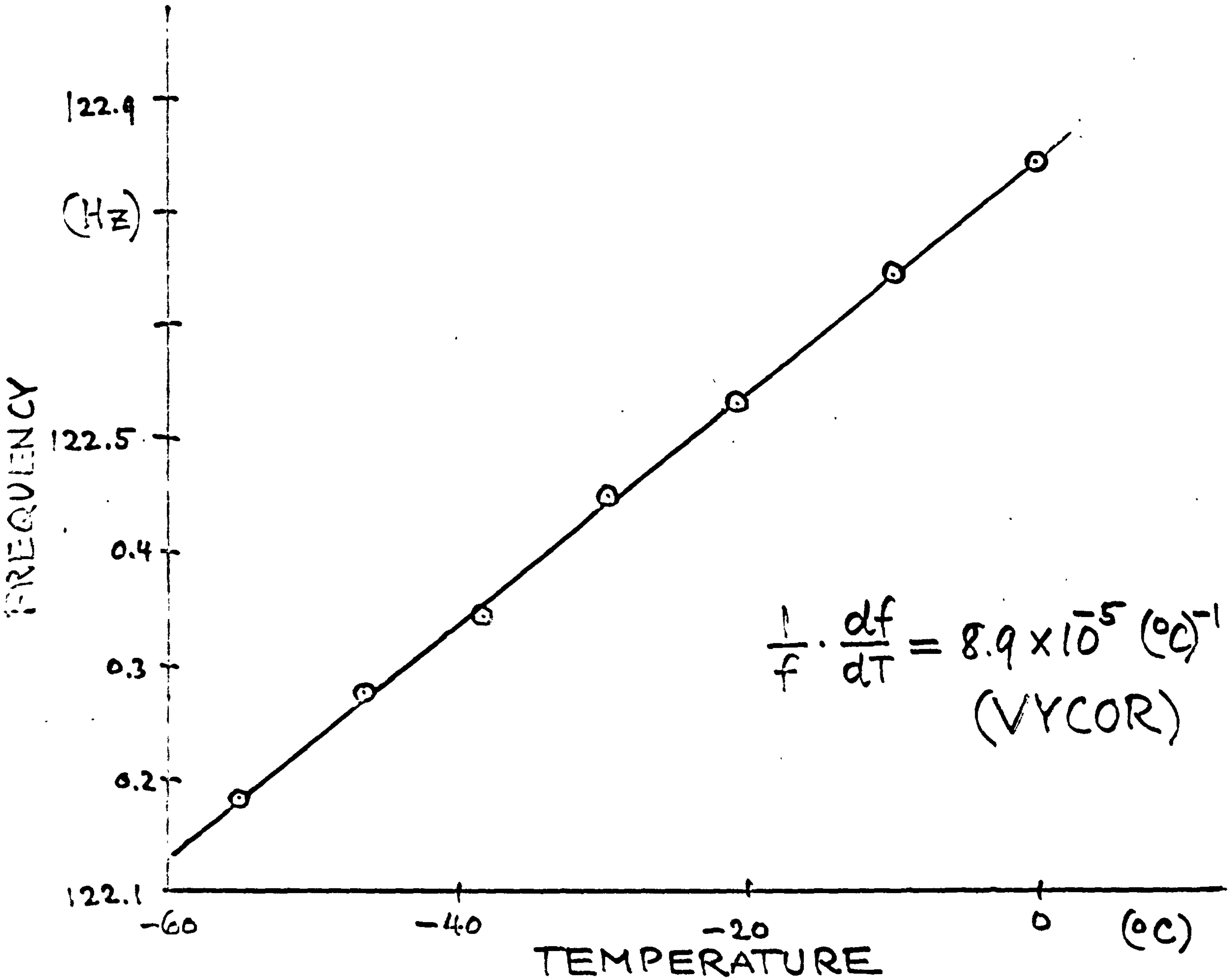

TEMPERATURE DEPENDENCE OF THE FREQUENCY

Figure 12

The temperature sensitivity, 1/f df/dT, is characteristic for the fiber material. It arises from the interplay of the expansion coefficient of the material, the taper of the fiber and the dependence of the elastic properties on temperature. It should be possible by utilization of these parameters to attenuate the temperature sensitivity of the device. This is important for high sensitivity devices. For a device with a frequency at 100 Hz, a frequency resolution of 10^{-4} Hz (10^{-9}g region) would require a temperature resolution of 0.01 °C. This amounts to an effective limit on the mass sensitivity of the device unless the temperature sensitivity is reduced. A significant reduction of temperature sensitivity can be accomplished in future units.

4.2 Temperature Transient Condition - When the fiber temperature is changing during frequency measurements, the relation between the temperature and the frequency becomes more complicated. Initially, it was felt that a thermistor placed near the fiber as shown in Figure 1 and Figure 13a would be representative of the fiber temperature since the essential parts of the device are housed in a metal cylinder which tends to minimize thermal gradients. Experimentally, however, it was found that this arrangement did not allow the achievement of a satisfactory relationship between temperature as indicated by the thermistor and frequency as determined by the fiber temperature under transient conditions.

A different approach was chosen. It was recognized that the heat

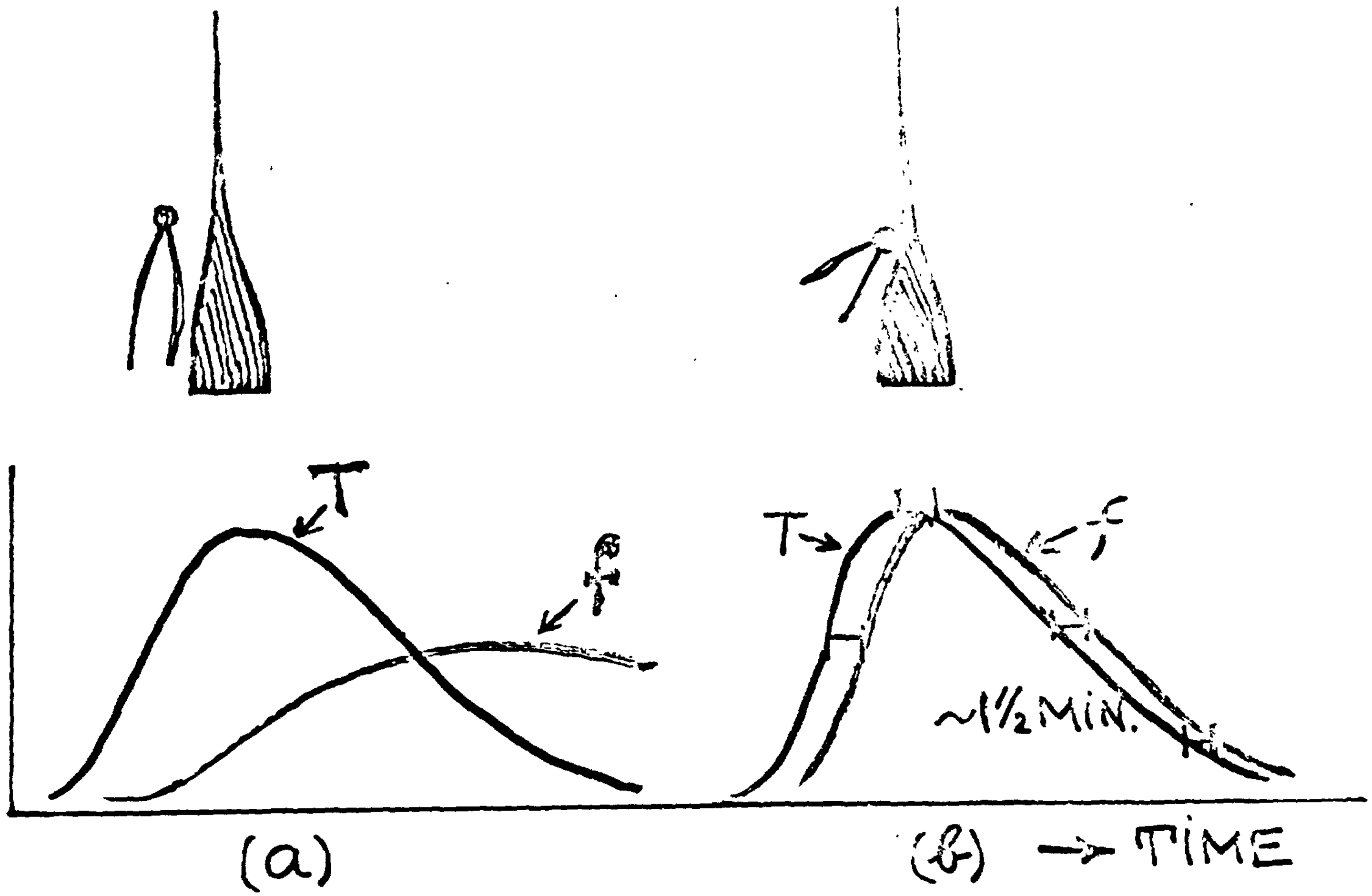

TEMPERATURE TRACKING

Figure 13

transfer to the fiber is controlled more by conduction through the fiber base than through the ambient gas (or radiational exchange in vacuum). Following this reasoning, the thermistor was epoxied to the fiber base as high as possible but in a position which did not interfere with the fiber oscillation. It was found that a straight-forward relationship exists between the thermistor temperature and fiber frequency. Essentially, the fiber frequency was found to lag the thermistor reading by a constant delay time (for a particular assembly) in the order of 1½ min. (See Figure 13b.)

The results for a typical device are shown in Figures 14 and 15 where frequency vs time and thermistor temperature vs time are plotted. From this data a delay of 1.4 min. was determined. In Figure 16 the reduced data is displayed showing that even for significantly different cooling and warm-up rates the correspondence between the thermistor reading and the fiber frequency is established to a high degree of accuracy. (We should emphasize that when conducting tests of this nature, care must be exercised due to the high mass sensitivity of the device to insure that no condensation or evaporation takes place on the substrate).

5. OPTIMIZATION OF TEOM PARAMETERS

In the construction of a TEOM, there are many parameters which can be varied in a controlled way. The device is capable of measuring both particulate and film depositions. The considerations for one type of measurement does not necessarily apply for the other. The emphasis

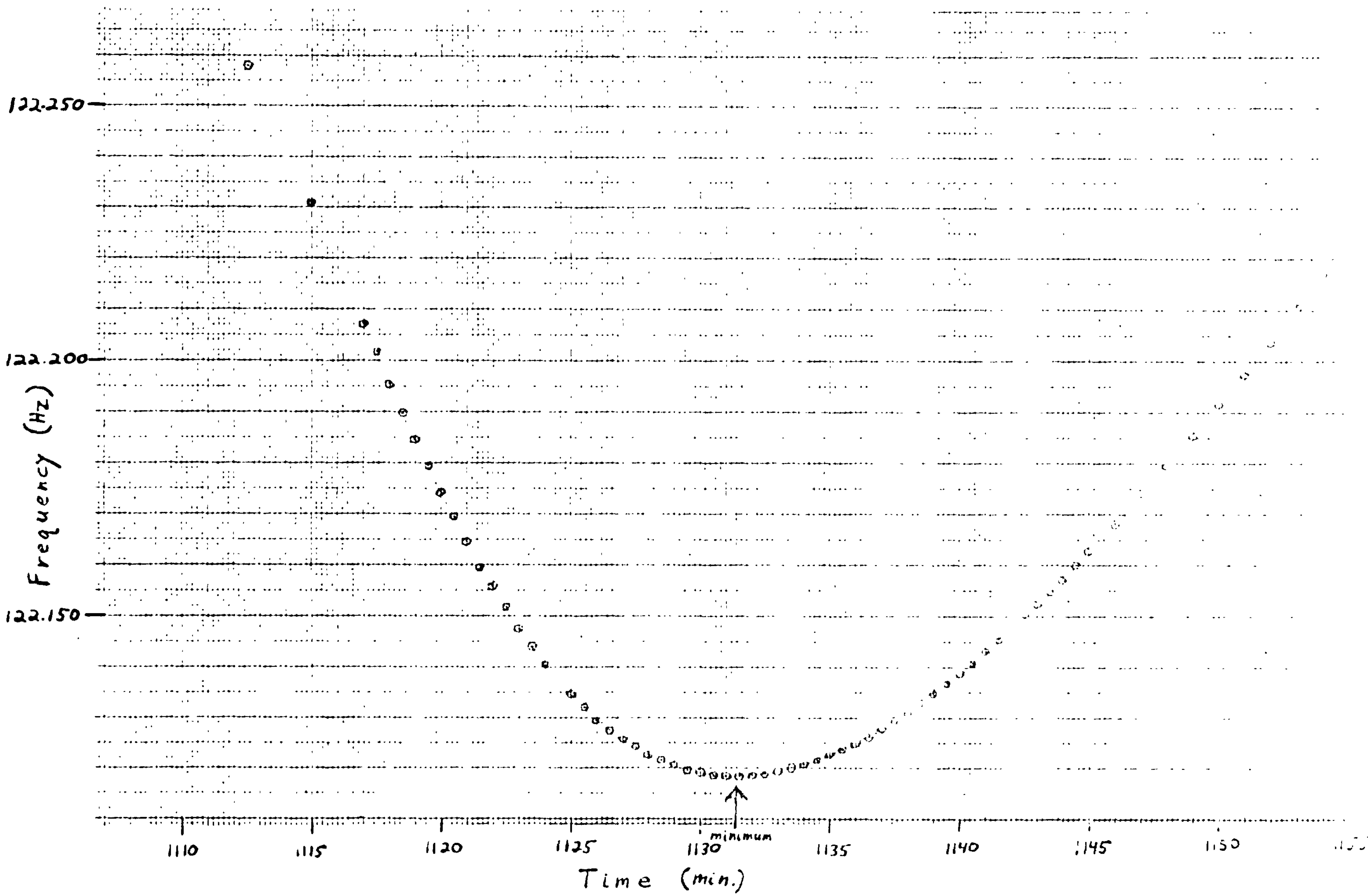

FREQUENCY VS. TIME

Figure 14

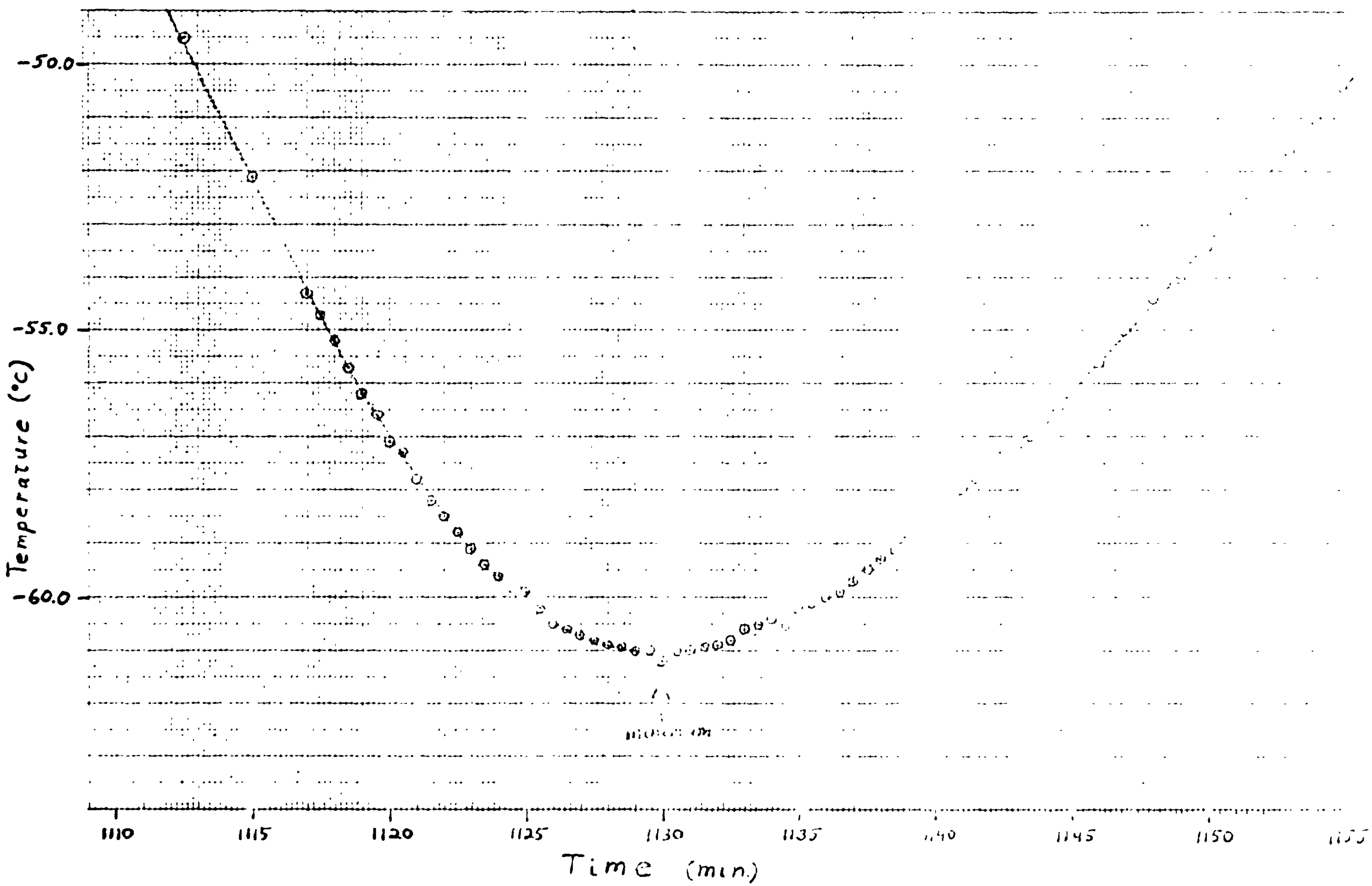

TEMPERATURE VS. TIME

Figure 15

COOLDOWN RATE 0° to -10°C 2.2 °C/min
WARMUP RATE -10° to 0°C 0.[illegible] °C/min

TEMPERATURE T (°C)	COOL DOWN TIME t_1	WARM UP TIME t_2	t_1 + 1.4 Min	t_2 + 1.4 Min	Hz f(t_1+1.4)	Hz f(t_2+1.4)
0°	1044.35	1335.85	1042.75	1336.7[illegible]	[illegible]22.74[illegible]	[illegible]
-10°	1045.4	1307.2	1046.8	1308.[illegible]	[illegible]2.64[illegible]	[illegible]
-55°	1117.75	1147.15	[illegible].15	[illegible]48.55	[illegible]	[illegible]

TEMPERATURE TRACKING

Figure 16

for the units which have been built for MSFC, however, has been placed on particulate measurements although they are usable for thin film deposition as well.

5.1 Frequency Considerations - The selection of an operating frequency for a TEOM involves a number of considerations. For the purpose of particulate measurments the overriding concern is on the surface acceleration which the substrate imparts to the deposited particles. The resulting force on the particles must be smaller than the adhesive force. Since the surface acceleration is proportional to f^2, a low frequency is to be preferred. Although this represents the major consideration for the frequency choice for these balances, other aspects should be considered as well. In particular, problems with external vibrational noise are best solved by utilization of a high resonant frequency for two reasons. First the power spectrum of local vibrational noise usually decreases with increasing frequency, and also, shock mounting of the device is much simpler for higher frequencies.

With these contradicting demands on the resonant frequency of the TEOM in mind, a compromise was made by selecting a frequency in the order of 100 Hz. This frequency is also sufficiently removed from 60 and 120 Hz which aids in the avoidance of 60 cycle pickup by electrical components of the device.

5.2 Fiber Parameterization - Fiber parameterization is important so that the operating characteristics (resonant frequency and sensitivity) of a particular fiber can be ascertained before it is considered for use and mounted in a balance. In order to accomplish this, the TEOM system was viewed as a vibrating system in which the resonant frequency is linked to the effective mass of the fiber and the mass load by the following expression:

$$f^2 \doteq \frac{K_o}{M+M_o} \qquad (K_o = \frac{K}{4\pi^2})$$

where K = force constant

M = mass load (substrate and added mass)

M_o= effective mass of the fiber

Using this approach, two basic fiber parameters are required, K_o and M_o. A technique has been developed to obtain these values for a given fiber.

In Figure 17 the dimensions of a typical fiber are shown. The fiber cross-section is elliptical so that oscillation will take place in one plane. The dimensions of the major axis and minor axis are shown as a function of length. The initial length of the fiber was in the order of 65mm and was cut in steps indicated by the dashed lines in the figure. After each cut, the natural resonance of the fiber was determined with and without a known mass load. From these two frequencies, K_o and M_o for that particular fiber length are readily computed. A plot of K_o vs length and M_o vs length are shown in Figures 18 and 19 respectively. K_o shows a strong dependence on fiber length

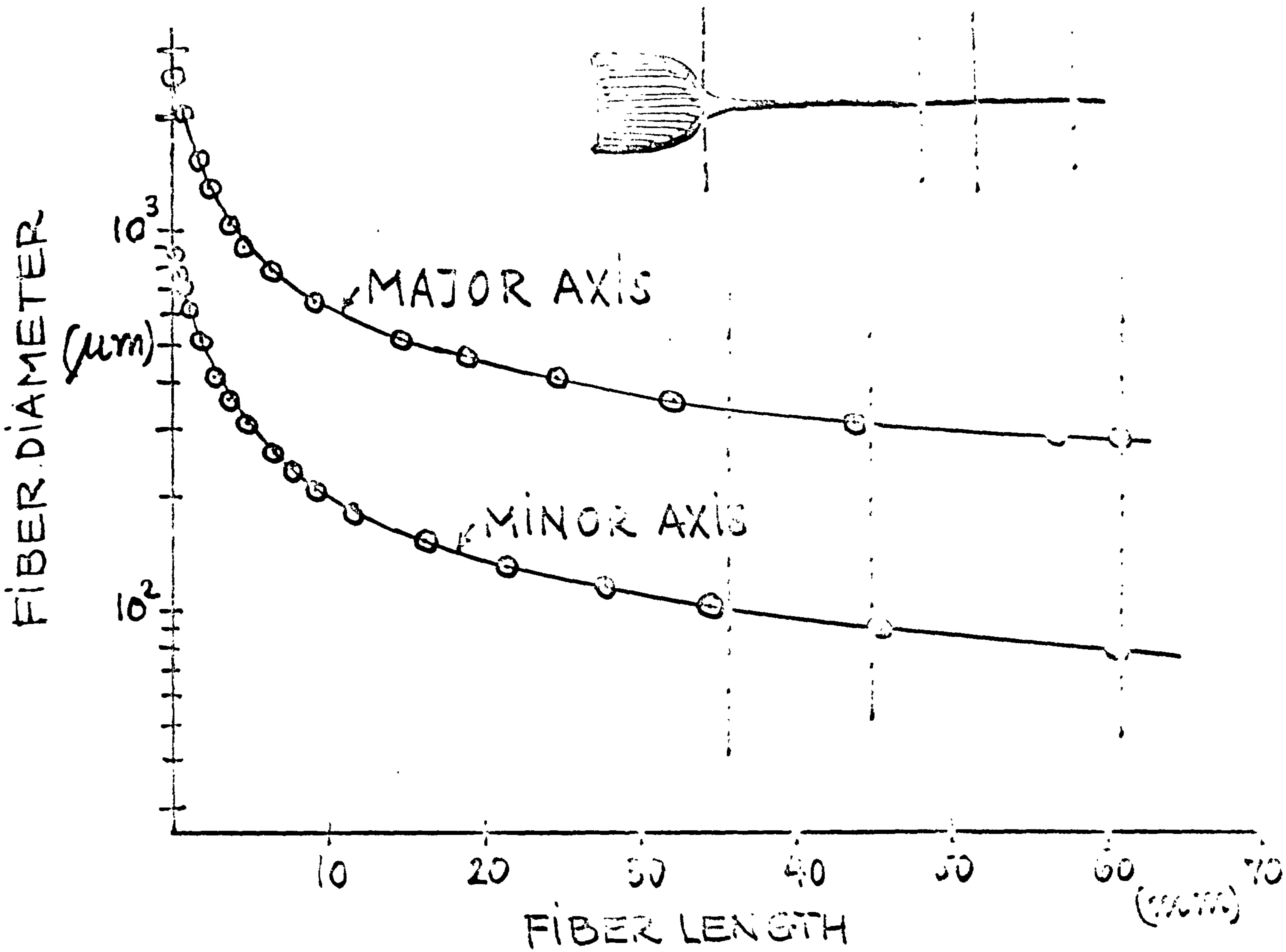

FIBER DIMENSIONS

Figure 17

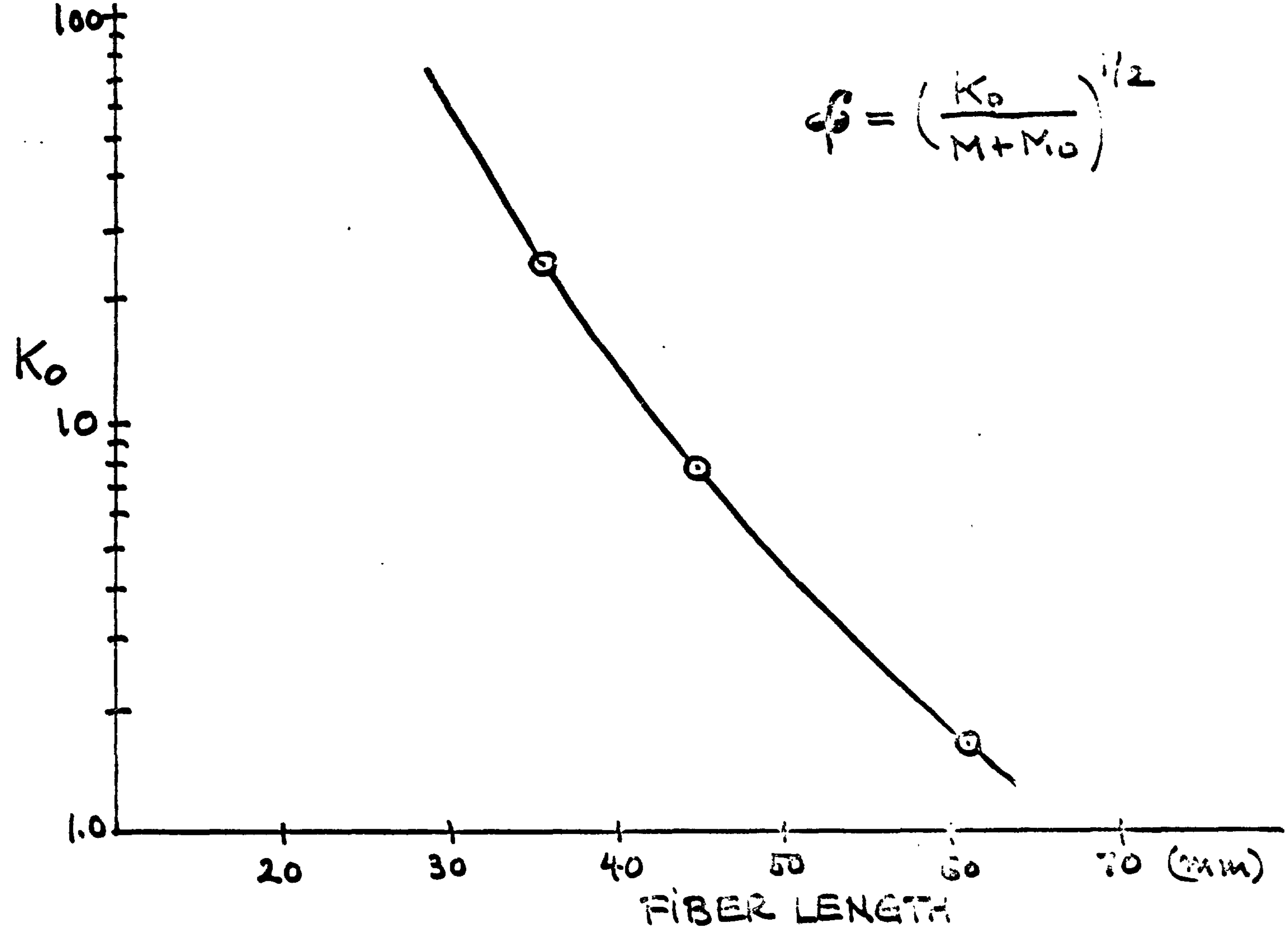

K_o VERSUS LENGTH

Figure 18

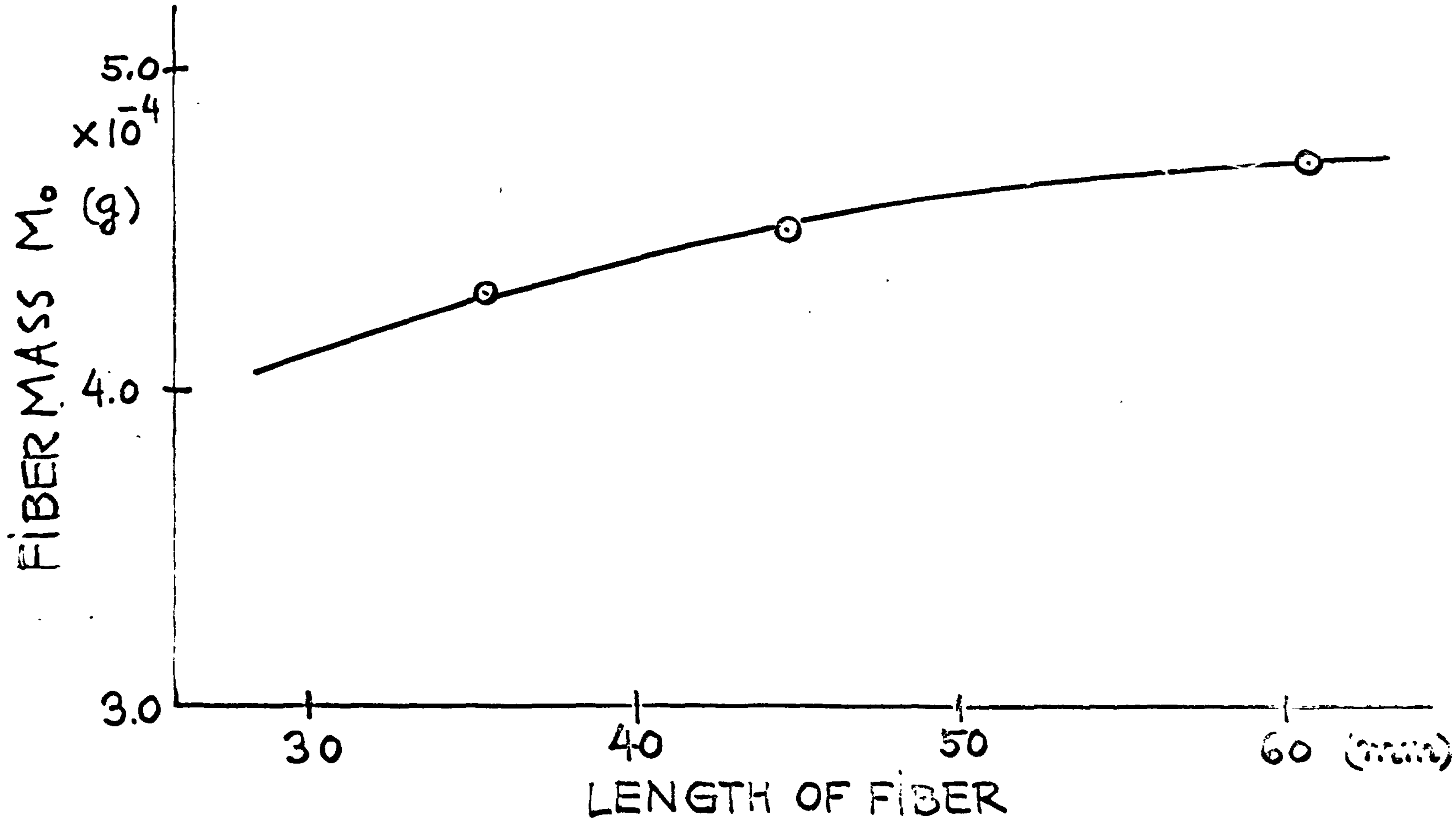

EFFECTIVE MASS, M_o, VS. FIBER LENGTH

Figure 19

while the effective mass M_o does not. These curves can be extrapolated to shorter lengths so that K_o and M_o (and therefore the frequency of fiber) can be predicted for any length and mass load. Equally important however is the determination of the sensitivity of the fiber. This can also be accomplished from these measurements.

The sensitivity of a fiber is related to the frequency shift, Δf, which results from a mass change, ΔM. However, it is not the absolute calue of Δf which is important here, i.e., a Δf of 10 Hz at an operating frequency of 10^3 Hz represents a lower sensitivity than a change of 10 Hz for a device operating at 20 Hz. For the TEOM system which uses period averaging counting techniques, any frequency can be determined to 1 part in the operating frequency of the crystal in the counter, typically 10 MHz, or 1 part in 10^7. Consequently, sensitivity is related to relative frequency change, $\Delta f/f$.

By differentiation of the above equation, one finds

$$\frac{df}{f} = -\frac{1}{2}\frac{dM}{M+M_o} .$$

This means that the sensitivity of a fiber depends only upon the effective mass of the fiber and the substrate mass. The K_o value serves only to set the operating frequency of the device. This can be shown graphically in Figure 20 where mass load is plotted as a function of frequency for a fiber whose length was chosen to provide three factors of ten changes in K_o.

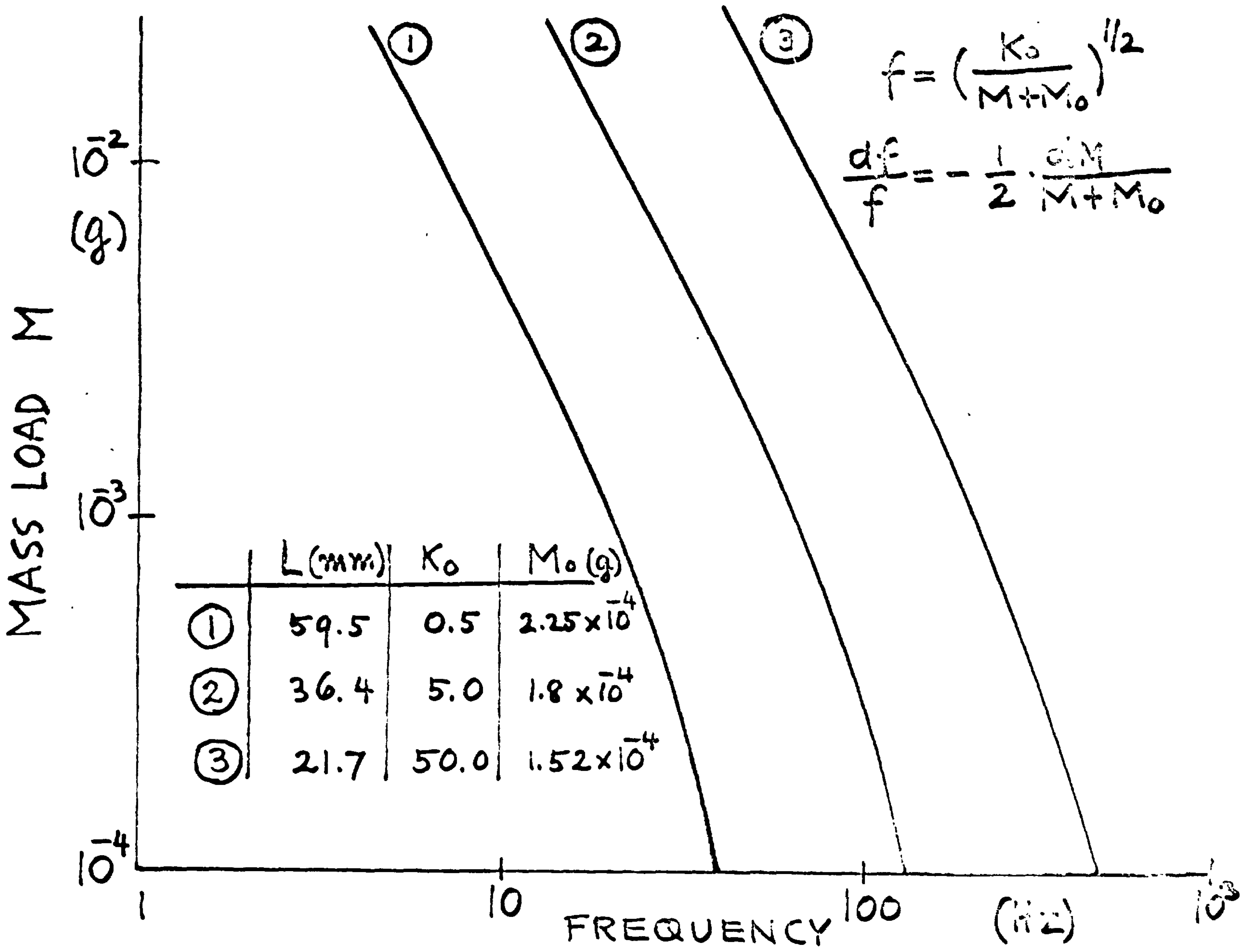

MASS LOAD VS. FREQUENCY
FOR VARIOUS K_o VALUES
Figure 20

5.3 <u>TEOM Sensitivity</u> - Since a TEOM can provide both particulate and thin film measurement capability, two types of sensitivity can be discriminated - a "particulate" sensitivity and an "area" sensitivity. The particulate sensitivity is defined as the relative frequency change per gram of added mass, $\frac{\Delta f}{f}/g$. For fibers with different M_o values the particulate sensitivity is shown in Figure 21 as a function of substrate mass. Also shown is the corresponding substrate diameter assuming a substrate area density of 3mg/cm^2. This corresponds to aluminum foil of 12.5μm thickness. For a fiber with $M_o = 3 \times 10^{-4}$g, a 5mm diameter substrate will yield a $\frac{\Delta f}{f}/g = 6 \times 10^2$. This means that for a device operating at 100 Hz, a Δf of 1 millihertz corresponds to a mass change of 1.7×10^{-8}g.

Similarly the area sensitivity can be defined as the relative change in frequency per gram per cm^2, $\frac{\Delta f}{f}/\frac{g}{cm^2}$, where the area is the area of the substrate. A series of curves for area sensitivity are shown in Figure 22. For a fiber with $M_o = 3 \times 10^{-4}$g and a 5mm substrate diameter, the area sensitivity, $\frac{\Delta f}{f}/\frac{g}{cm^2} = 120$. Operating at 100 Hz, a 1 millihertz frequency change corresponds to 8.3×10^{-8}g/cm^2.

Although the original microbalance delivered to MSFC had a substrate diameter of 10 mm, 5mm substrates have now been chosen for the most recent instruments delivered to MSFC (October 1, 1976). By examination of the sensitivity curves, a change from 10 mm diameter to 5 mm increases the particulate sensitivity by about a factor of 3 while

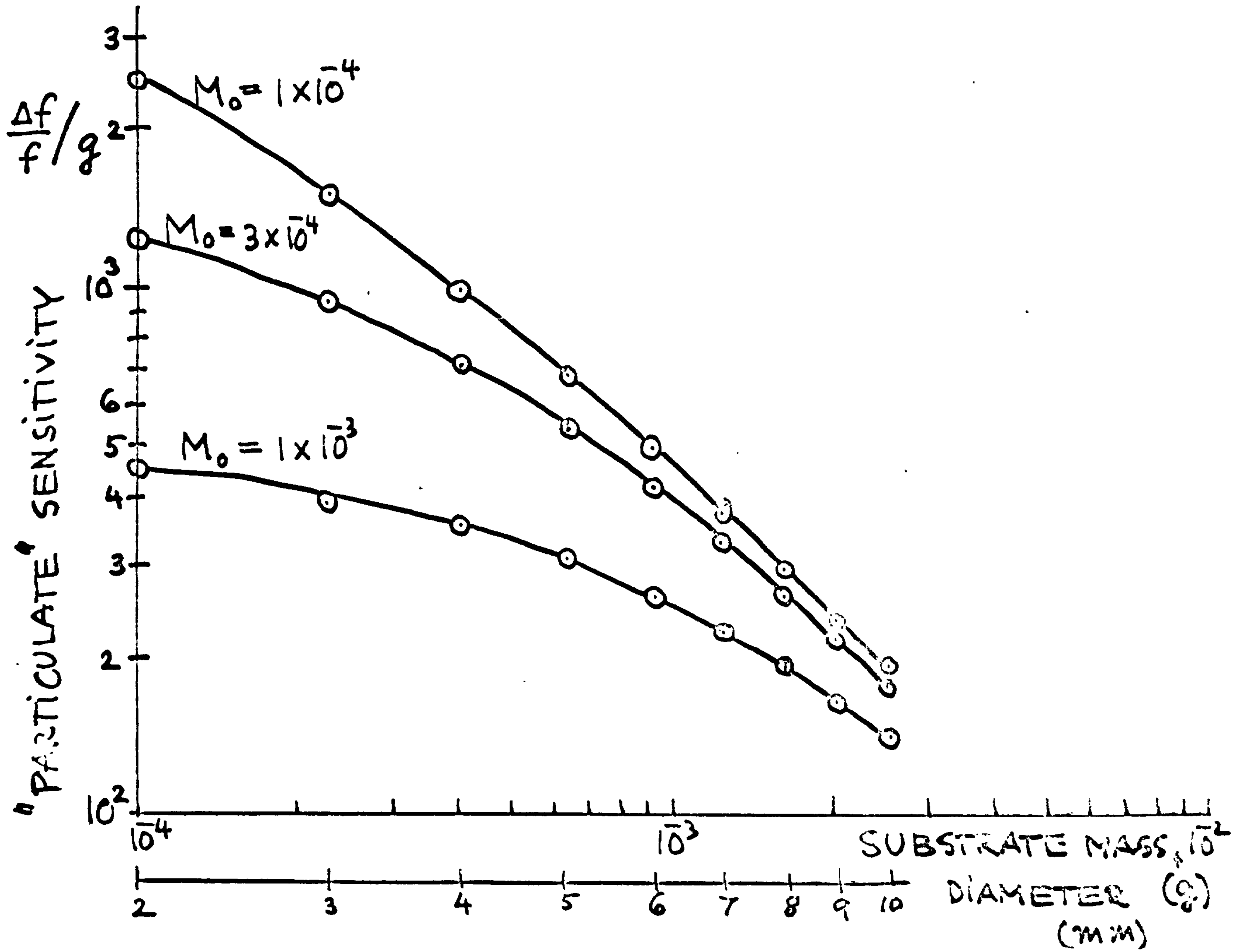

"Particulate" Sensitivity

Figure 21

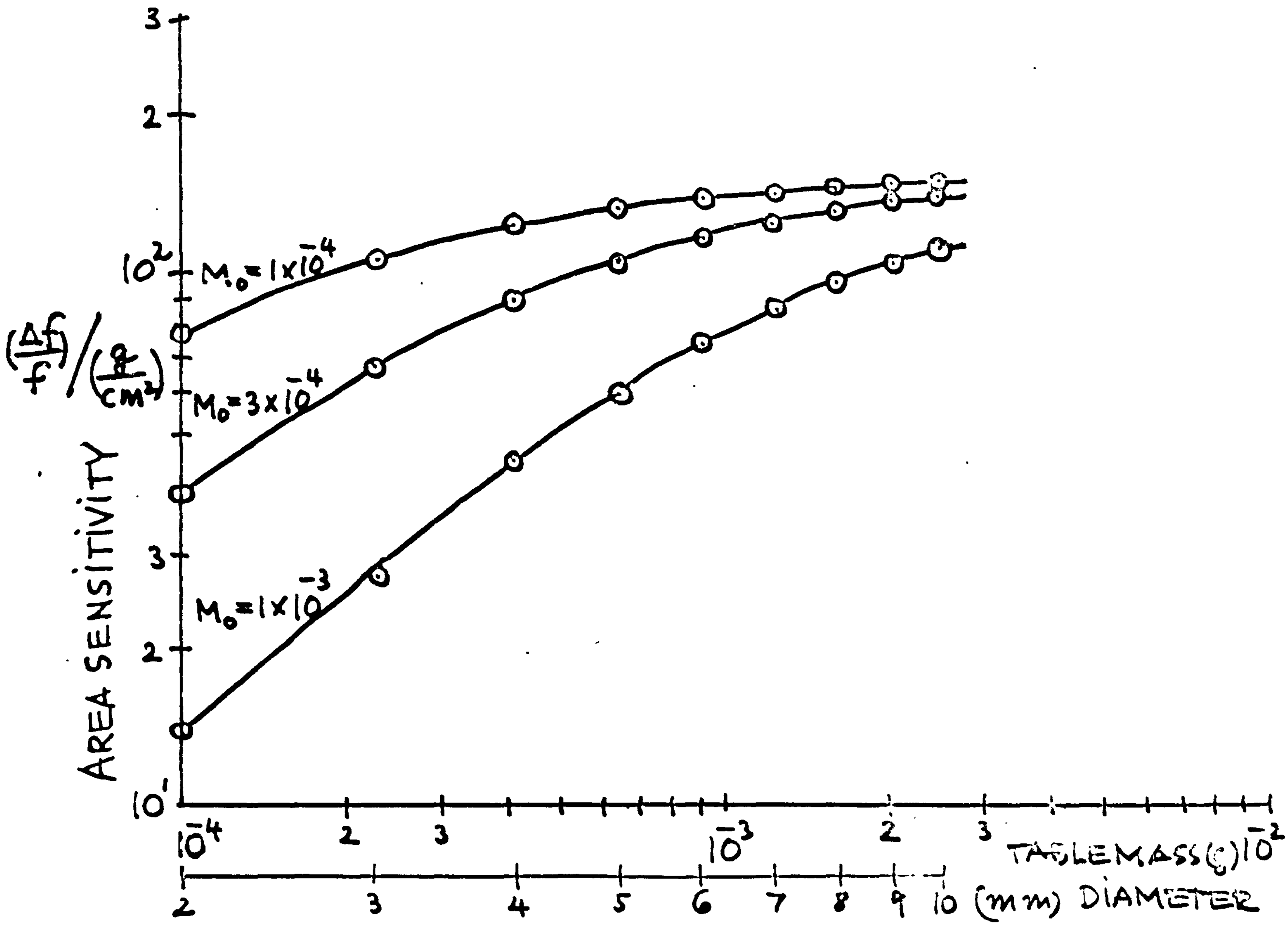

AREA SENSITIVITY

Figure 22

the area sensitivity suffers by a decline of only 30%.

5.4 Substrate Design - The original substrate for the TEOM was mica, but it is one of the advantages of the TEOM that many other substrates can be used as well. For the present systems delivered to MSFC aluminum substrates are used. In order to improve the stiffness of the aluminum a conical structure was chosen as illustrated in Figure 23. The dimensions have been computed in such a way so that the point where the table is attached to the fiber corresponds to the center of mass of the substrate. This helps to prevent the development of moments during fiber oscillation.

6. DESCRIPTION AND PERFORMANCE CHARACTERISTICS OF THE TEOM INSTRUMENTATION

Under the second phase of this contract three improved TEOM units have been delivered along with a functional prototype of a total electronics package.

Operating instructions are supplied in Section 8.

All three balances are interchangeable with the electronics package and have been designed and constructed to perform with almost identical performance characteristics. The units have aluminum substrates as illustrated in Figure 23. These substrates are attached to the fiber with nitrocellulose and have been designed with exchangeability in mind. The exchange procedure for the time being is a relatively critical manual operation and has not yet been automated. It is therefore

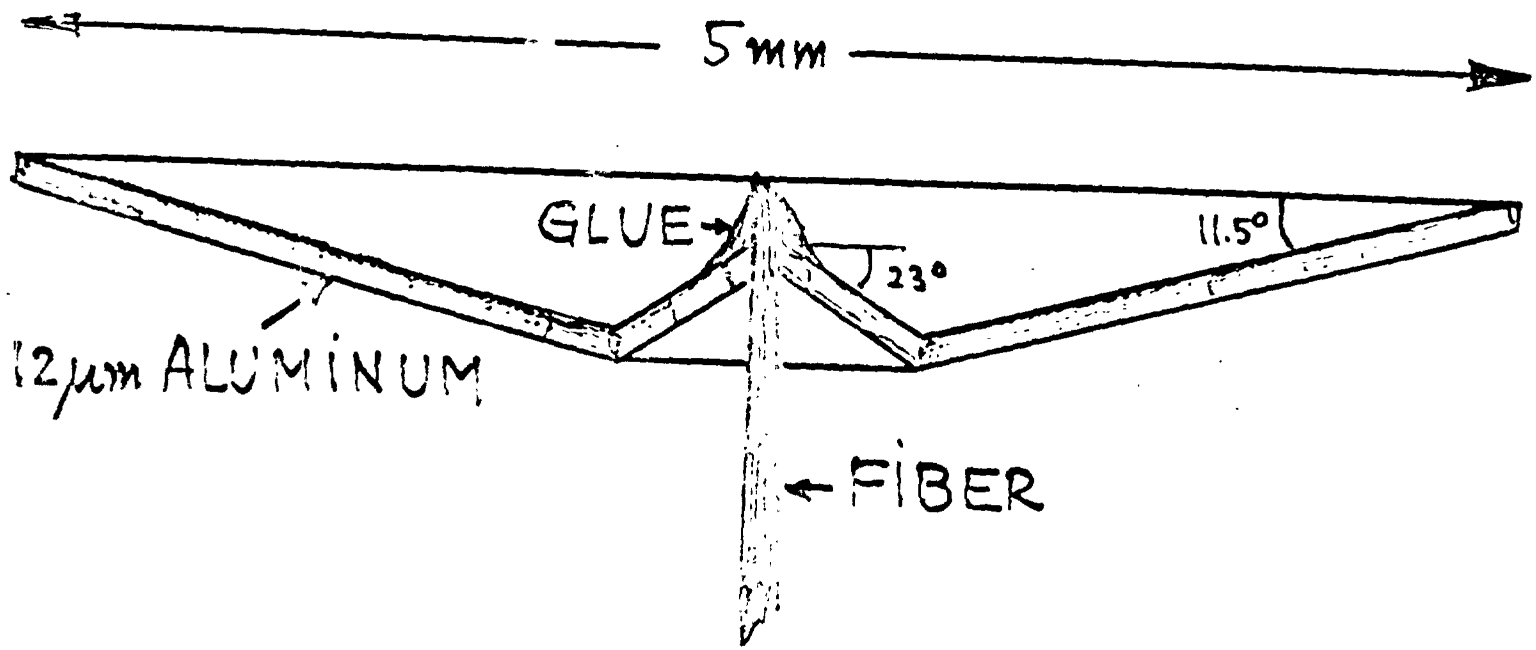

TABLE CONFIGURATION

Figure 23

recommend that no substrate exchange be attempted by MSFC personnel.

The three units (G, H and I) are almost three times as sensitive as the unit delivered last October (1975) as a result of the improvements during the second phase of this contract. The operational characteristics are summarized in the following table.

Basic TEOM Data for the Supplied Units G, H and I

Unit	G	H	I
K_o (g Hz^2)	10.404	10.876	10.175
M_o (g)	1.021×10^{-3}	1.026×10^{-3}	1.011×10^{-3}
τ (min)	1.7	1.8	1.5
$1/f \frac{\Delta f}{\Delta T}$ ($^oC^{-1}$)	9.0×10^{-5}	9.0×10^{-5}	9.0×10^{-5}

Under laboratory bench conditions the units demonstrate a frequency resolution of better than 10^{-4}Hz. The packaged electronics however has been designed for millihertz resolution as per the contract specifications and available funding. Millihertz resolution at the resonant frequency of the units is equivalent to less than 2×10^{-8}g.

7. RECOMMENDATIONS

The following recommendations are made for the further development of the TEOM.

A) Stabilization under varying "Q". If the TEOM is to be operated under different pressure situations, then a means to automatically compensate the drive level to the fiber should be incorporated.

B) Easier exhangeability of substrates Although substrates can be exchanged manually at present, an automatic or semi-automatic device should be available to make this task easier.

C) Incorporation of the TEOM with an impactor. The current device is intended as a dust fall monitor for shuttle, but it also holds great promise as the detecting element in a multistage impactor arrangement which would allow size distribution and mass concentration measurements of airborne particulates.

D) Electronics optimization and packaging. The electronics package delivered to MSFC (6"x6"x6") is larger than necessary and should be reduced. Also a means to provide a 90° phase shifted drive signal over a wide frequency range should be introduced. Other features such as an LED readout of frequency and logic to convert frequency measurements into mass should also be incorporated if the electronics package is to be used in other than a shuttle compatable system.

E) For mass measurements at either high or low temperatures (i.e. beyond the operating limits of the solid state optical components) the system can be designed such that the optical components are removed from the immediate vicinity of the oscillating element and thus protected from extremes in temperature. For very high temperature applications, other fiber materials (such as sapphire) may prove desirable.

8. OPERATING INSTRUCTIONS FOR THE FUNCTIONAL PROTOTYPE OF THE TEOM DUST FALL MONITOR

8.1 Introduction - The TEOM monitoring system is designed to measure mass depositions on a 5mm diamter aluminum substrate. This surface is located at the end of a specially tapered fiber which is maintained in oscillation by a photo-optical-electrostatic feedback system (see Figure 4). The frequency of the oscillation of the tapered fiber is used to determine the mass on the collecting surface. The microbalance is housed in a cylindrical envelope (approximately 1½" in diameter and 4" long). The cap on the top of the cylinder can be removed to open the unit and expose the substrate. The bottom of the balance is a modified MS series connector which fits into the electronics package.

All the necessary support electronics is housed in 6"x6"x6" package. Included in the package is an amplifier, period averaging frequency counter, temperature monitor, power supplies and "handshake" control circuitry.

8.2 Operation Instructions - See Figures 24, 25 and 26 for location of the connectors referred to below.

1. Plug one of the three interchangeable TEOM units in the connector J1 on top of the electronics package, or supply a connection with a cable between the electronics package and a TEOM unit. (The phototransitor output line must be shielded. A schematic is included which indicates the appropriate pin connections).

2. Wherever the TEOM unit is operated provide at least a 1" to 2" foam pad for simple shock mounting.

3. Provide 28 vdc to power plug, J3, of the electronics package.

4. Connect readout devices to connector J2 for data retrieval (If necessary a voltmeter can be used to determine the state of each output pin). Data output for frequency information is composed of 24 bits comprising three 8 bit words, tristate CMOS output TTL compatable. Temperature output is 0-5 vdc analog. (A digital voltmeter is recommended for this measurement).

5. To turn the unit on supply a +28 v pulse to pin f of connector J2. To turn off supply a +28 v pulse to pin g. A power-on indicator light is located next to connector J1.

6. If desired, the output of the phototransistor which is representative of the mechanical oscillation of the fiber can be measured with an oscilloscope at the BNC connector, J5. This signal level is approximately 0.15 to 0.2 v p-p. The fiber drive signal (amplifier output) can be monitored at the BNC connector, J4. This signal level is usually in the order of 100 v p-p depending on the gain setting of the amplified. This

gain has been preset and should not ordinarily be tampered with. The amplifier gain is controlled by a trimpot which is adjusted until the sinusoidal phototransistor signal is within the above mentioned operating range. Do not change gain settings during the time measurements are in progress. At no time should the unit be allowed to operate if the phototransistor signal shows any discountinuities or spikes. This would occur if the fiber and/or substrate is hitting against something usually due to an excessive amplitude. See Figure 25 for the position of J4, J5 and the amplitude gain adjustment.

8.3 Frequency Interpretation

Connector J2

Pin		n
A	corresponds to 2^n	23
B		22
C		21
D		20
.		.
.		.
.		.
X		3
Y		2
Z		1
a		0

$N = Ax2^{23} + Bx2^{22} + Cx2^{21} +$---------- where A, B, C, etc. are either 0 or 1. N = total number of 10 MHz periods within 100 TEOM cycles. Therefore, frequency of TEOM oscillation, $f = \frac{1}{N} \times 10^9$ (1)

8.4 Temperature Calibration -

A Fenwal UUB31J1 thermistor provided in the TEOM units is used to determine the temperature of the oscillating element. The temperature is represented by an output voltage at pin h of connector J2. The resistance value of the thermistor is determined by this voltage by the following relation:

$$R_{thermistor} = \frac{1.60 \times 10^5}{(3.023 \times 10^2)\ v^{-1} - 1} \qquad (2)$$

The resistance of the thermistor vs temperature is provided in the appended table taken from the data sheet provided by the manufacturer. (See page 59.)

8.5 Frequency and Temperature Correlation -

In all the supplied TEOM units the frequency changes as a function of temperature. The relation between corresponding temperature change, ΔT, and frequency change, Δf, is given by the relation

$$\frac{1}{f}\,\frac{\Delta f}{\Delta T} = 9.0 \times 10^{-5} \qquad (3)$$

Through experimentation, it has been found that during temperature transients the frequency lags behind the temperature measurement supplied by the thermistor by a constant delay time, τ, which is listed for the individual units in the TEOM data table.

Since the electronics package provides continuous temperature information but discontinuous frequency information, care must be excercised in correlating frequency measurements with temperature readings. Keep in mind that the readout time for frequency is not the time when the frequency has been measured, and also remember that corresponding frequencies and temperatures are delayed by τ where the frequency lags behind the temperature. By tailoring the delay time between the sets of handshake pulses to coincide with τ for a given unit, one can make the temperature and frequency correlation most convenient.

In equation 3, ΔF and ΔT pertain to corresponding quantities, i.e. ΔF is measured τ minutes after the measurement of ΔT. In a steady-state condition this correction can obviously be disregarded.

8.6 Mass Evaluation

The relationship between the mass on the substrate and the frequency of the TEOM is given by the relation:

$$m = \frac{K_o}{f^2} - M_o \qquad (4)$$

where K_o is proportional to the restoring force of the fiber, M_o is the effective mass of the fiber and substrate table, and f is corrected to a reference temperature, T_o.

Since K_o and M_o are constants for a particular fiber the mass, m, on the table can be determined. To determine a mass added on the substrate at any particular time, first measure the frequency without the mass or at the start of a deposition period. Use this frequency to compute any mass residue (or loss), m_r, associated with the substrate which is now acting as a mass "background". With the mass to be measured on the substrate, determine the new frequency and compute a mass, m'. The added mass is then simply,

$$m = m' - m_r \qquad (5)$$

8.7 Mechanical Considerations - (Refer to Figures 27, 28, and 29)

The TEOM units are built with exchangability of substrates and fibers in mind.

The aluminum substrates are attached to the fibers with a minute quantity of nitrocellulose which is soluble in a variety of solvents. To exchange the table, the nitrocellulose is dissolved and the substrate can be removed. A new substrate can then be placed on the fiber. Since this procedure has not yet been automated in these units, it is strongly recommended that this exchange of tables be carried out by the manufacturer. Substrates may be cleaned by placing a small drop of isopropyl alcohol on them and immediately drawing off the fluid carefully with a corner of a piece of absorbent tissue paper.

Fibers can also be removed and replaced. First unsolder fiber drive and thermistor connections at pins F, D, and at the ground line from pin H in the unit. Remove the capacitor plate holder on the si e of the slit in the top plate of the unit. On the same side, remove the photo-optics alignment bracket. Carefully unscrew the fiber platform and lift it with the fiber out of the unit while carefully guiding the fiber through the slot in the top plate. Fibers should not be interchanged from unit to unit. It is again recommended that fiber removal and exchange be left to the manufacturer.

8.8 Basic TEOM Data for the Supplied Units G, H. and I -

Unit	G	H	I
K_o (g Hz^2)	10.404	10.876	10.175
M_o (g)	1.021×10^{-3}	1.026×10^{-3}	1.011×10^{-3}
τ (min)	1.7	1.8	1.5
$1/f \frac{\Delta f}{\Delta T}$ ($^\circ C^{-1}$)	9.0×10^{-5}	9.0×10^{-5}	9.0×10^{-5}

NOTE: The TEOM units can be used within a temperature range of from +40°C to -40°C. The electronics package is designed only as a functional prototype and it is recommended that it be utilized only under "on the bench" laboratory conditions. With the functional prototype electronics, no provision has been made for automatic gain control or automatic phase corrections for the driving signal. Consequently, the amplitude of oscillation will decrease and oscillation may stop if masses greater than 0.5mg are placed on the substrates. The balances themselves are capable of weighing a milligram load with appropriate gain and phase adjustments.

8.9 Trouble Shooting Hints

If the combined TEOM - Electronics package system is not functioning, the first step is to isolate whether the problem lies in the TEOM unit or the electronics package. Schematics for the electronics package are provided at the back of this manual.

1. With the TEOM removed from J1 check voltages at the connector.

Pin	J	-100 vdc
	K	+100 vdc
	E	+ 5 vdc

2. Insert a 100 Hz sine ware signal (0.1 - 0.2 v p-p) at pin A on J1. Observe output at pin F. This should be a 50 - 200 v p-p signal which is phase-shifted 90° from the input signal at pin A.

3. With that test signal, check the operation of the counter at connector J2 as per operating instructions (Sections 8.2 and 8.3).

4. If the electronics package checks out correctly, the problem is most likely in the TEOM unit or in any extension cables used with it. Do not attempt to work on the TEOM unit. Return it for any repairs.

8.10 PARTS LIST

TEOM Units*

LED - Phototransistor	GE H13A1
Thermistor	Fenwal UUB31J1

Electronics Package

All components within the electronics package are indicated on the schematics.

* These units should be returned for any repairs and/or modifications. No attempt should be made to work on these units.

8.11 CAUTION

1. Although the TEOM units are vacuum compatable, no provision is made in the electronics of the functional prototype to compensate for the change in damping at reduced pressures. Damage to the fiber and/or substrate may result through an extreme overdriven situation. Do not operate the TEOM with this electronics package under reduced pressure.

2. Keep unit capped when not in use.

3. Do not clean substrate in solvents that will dissolve or soften nitrocellulose.

4. Temperature stability measurements are only valid if the units are operated in a controlled environment which insures that no mass is evaporating or condensing on the substrate. These are extremely sensitive units, 0.001 Hz corresponds to 2×10^{-8}g.

Temperature vs. Thermistor Resistance

COLOR CODE GREEN/BLUE DOT

Temp °C	Resist Ω	Temp °C	Resist Ω	Temp °C	Resist Ω	Temp °C	Resist Ω
-80	229,000	-6	3,489	68	244.8	142	40.2
-79	213,100	-5	3,339	69	237.8	143	39.4
-78	198,500	-4	3,196	70	231.0	144	38.6
-77	184,900	-3	3,061	71	224.5	145	37.8
-76	172,400	-2	2,931	72	218.2	146	37.0
-75	160,800	-1	2,808	73	212.0	147	36.3
-74	150,000	0	2,691	74	206.1	148	35.6
-73	140,000	1	2,579	75	200.4	149	34.9
-72	130,800	2	2,472	76	194.9	150	34.2
-71	122,200	3	2,370	77	189.5		
-70	114,300	4	2,273	78	184.3		
-69	106,900	5	2,181	79	179.3		
-68	100,000	6	2,093	80	174.5		
-67	93,630	7	2,009	81	169.8		
-66	87,700	8	1,928	82	165.2		
-65	82,170	9	1,852	83	160.8		
-64	77,040	10	1,779	84	156.6		
-63	72,250	11	1,709	85	152.4		
-62	67,800	12	1,642	86	148.4		
-61	63,640	13	1,578	87	144.5		
-60	59,770	14	1,518	88	140.8		
-59	56,160	15	1,459	89	137.1		
-58	52,780	16	1,404	90	133.6		
-57	49,630	17	1,351	91	130.2		
-56	46,690	18	1,300	92	126.8		
-55	43,940	19	1,251	93	123.6		
-54	41,370	20	1,204	94	120.5		
-53	38,970	21	1,160	95	117.5		
-52	36,720	22	1,117	96	114.5		
-51	34,620	23	1,076	97	111.7		
-50	32,640	24	1,037	98	108.9		
-49	30,800	25	1,000	99	106.2		
-48	29,050	26	963.4	100	103.6		
-47	27,440	27	925.9	101	101.1		
-46	25,920	28	895.9	102	98.6		
-45	24,490	29	864.1	103	96.2		
-44	23,150	30	833.7	104	93.9		
-43	21,890	31	804.5	105	91.6		
-42	20,700	32	776.5	106	89.5		
-41	19,590	33	749.6	107	87.3		
-40	18,550	34	723.8	108	85.3		
-39	17,560	35	699.0	109	83.2		
-38	16,640	36	675.2	110	81.3		
-37	15,770	37	652.4	111	79.4		
-36	14,940	38	630.4	112	77.6		
-35	14,170	39	609.3	113	75.8		
-34	13,440	40	589.0	114	74.0		
-33	12,760	41	569.5	115	72.3		
-32	12,110	42	550.7	116	70.7		
-31	11,500	43	532.7	117	69.1		
-30	10,920	44	515.3	118	67.5		
-29	10,380	45	498.6	119	66.0		
-28	9,866	46	482.5	120	64.5		
-27	9,381	47	467.0	121	63.1		
-26	8,922	48	452.1	122	61.7		
-25	8,489	49	437.8	123	60.3		
-24	8,079	50	423.9	124	59.0		
-23	7,692	51	410.6	125	57.7		
-22	7,325	52	397.8	126	56.4		
-21	6,978	53	385.4	127	55.2		
-20	6,649	54	373.5	128	54.0		
-19	6,338	55	362.0	129	52.9		
-18	6,043	56	351.0	130	51.7		
-17	5,764	57	340.3	131	50.6		
-16	5,499	58	330.0	132	49.5		
-15	5,248	59	320.1	133	48.5		
-14	5,009	60	310.5	134	47.5		
-13	4,783	61	301.2	135	46.5		
-12	4,569	62	292.3	136	45.5		
-11	4,365	63	283.7	137	44.6		
-10	4,172	64	275.3	138	43.6		
-9	3,988	65	267.3	139	42.7		
-8	3,813	66	259.3	140	41.9		
-7	3,647	67	252.0	141	41.0		

PROTOTYPE TEOM AND CONTROL ELECTRONICS BOX ASSEMBLY - THREE QUARTER VIEW

Figure 24

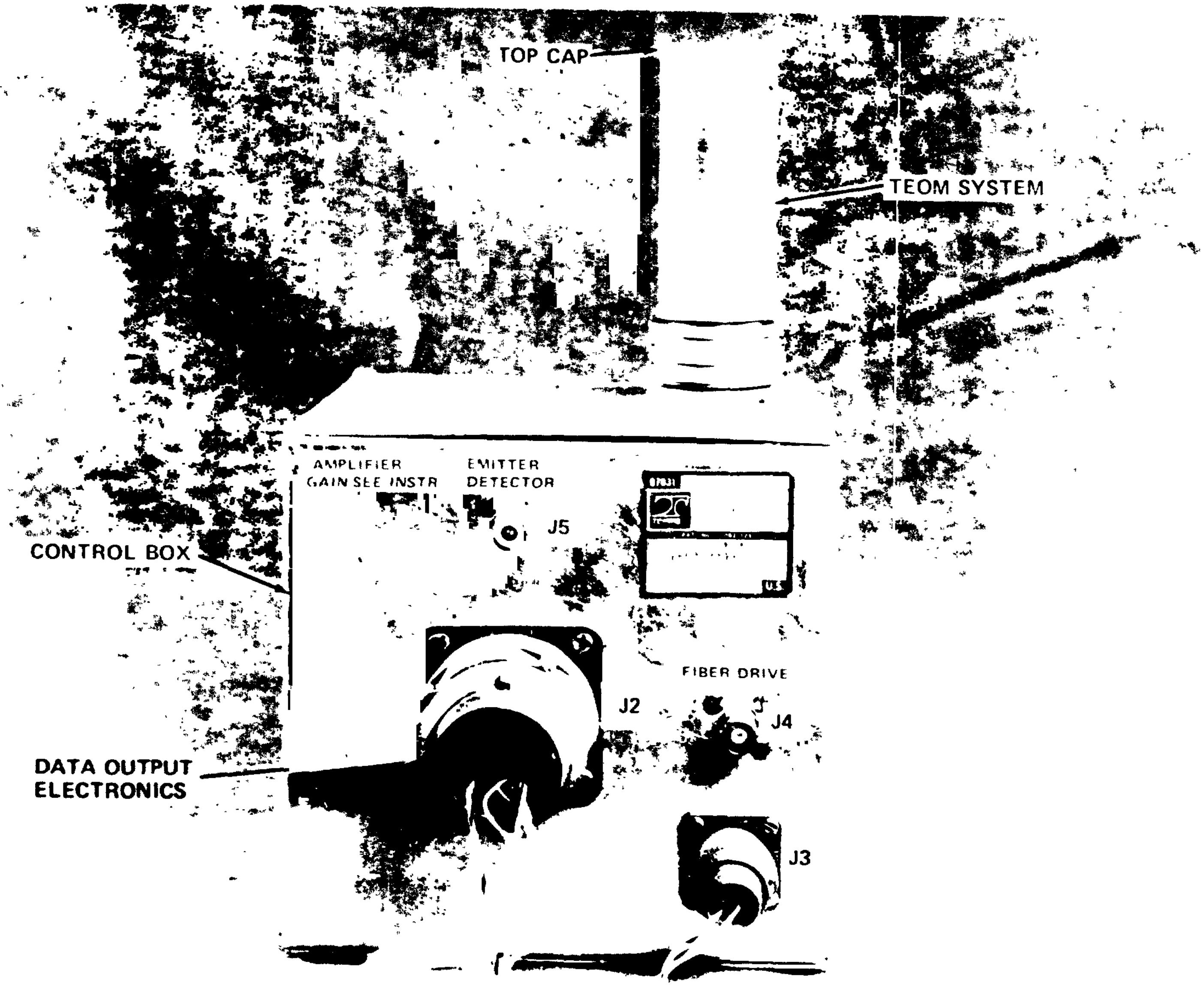

PROTOTYPE TEOM SYSTEM AND CONTROL ELECTRONICS BOX ASSEMBLY - FRONT VIEW

Figure 25

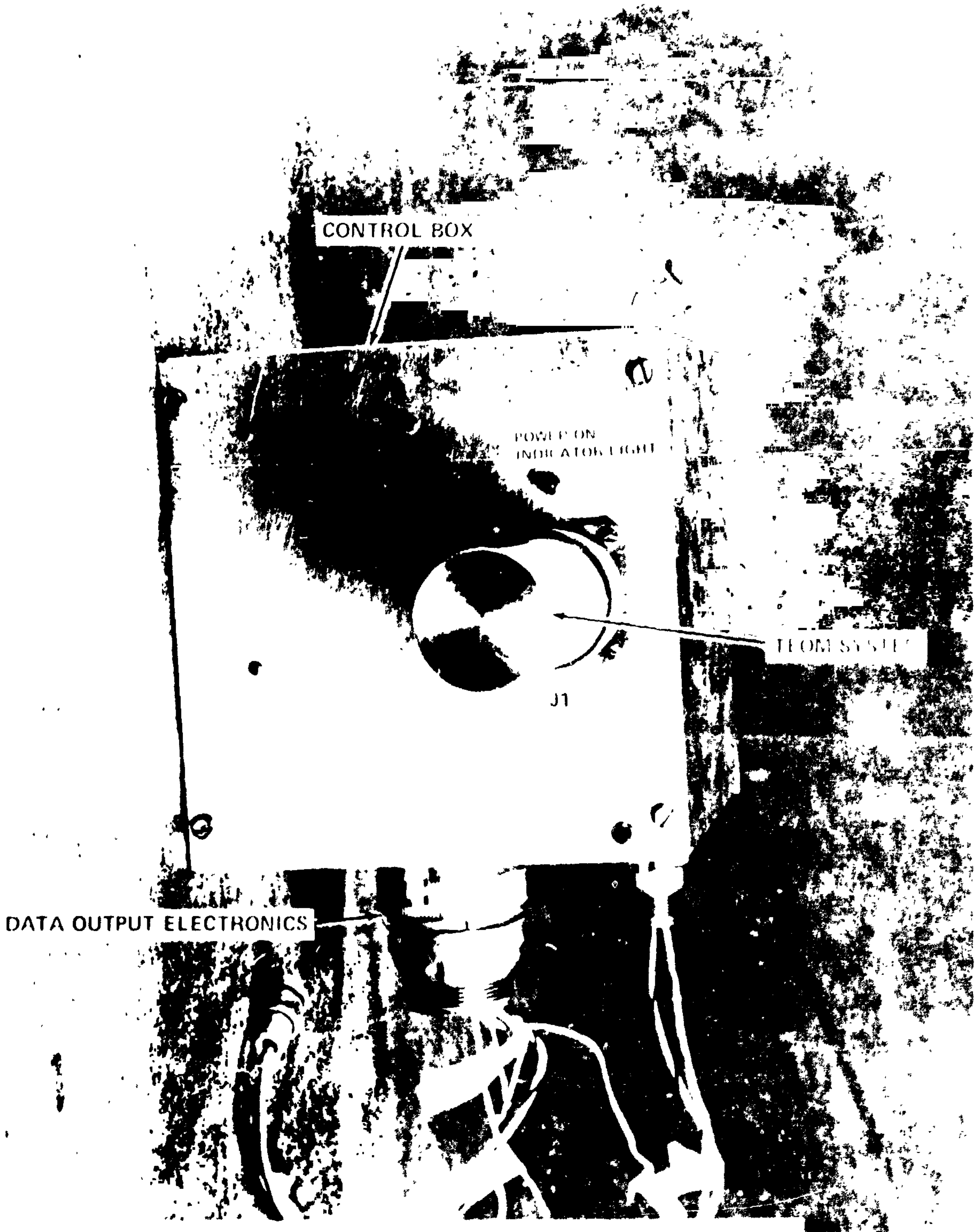

PROTOTYPE TEOM SYSTEM AND CONTROL ELECTRONICS
BOX ASSEMBLY TOP VIEW

Figure 2

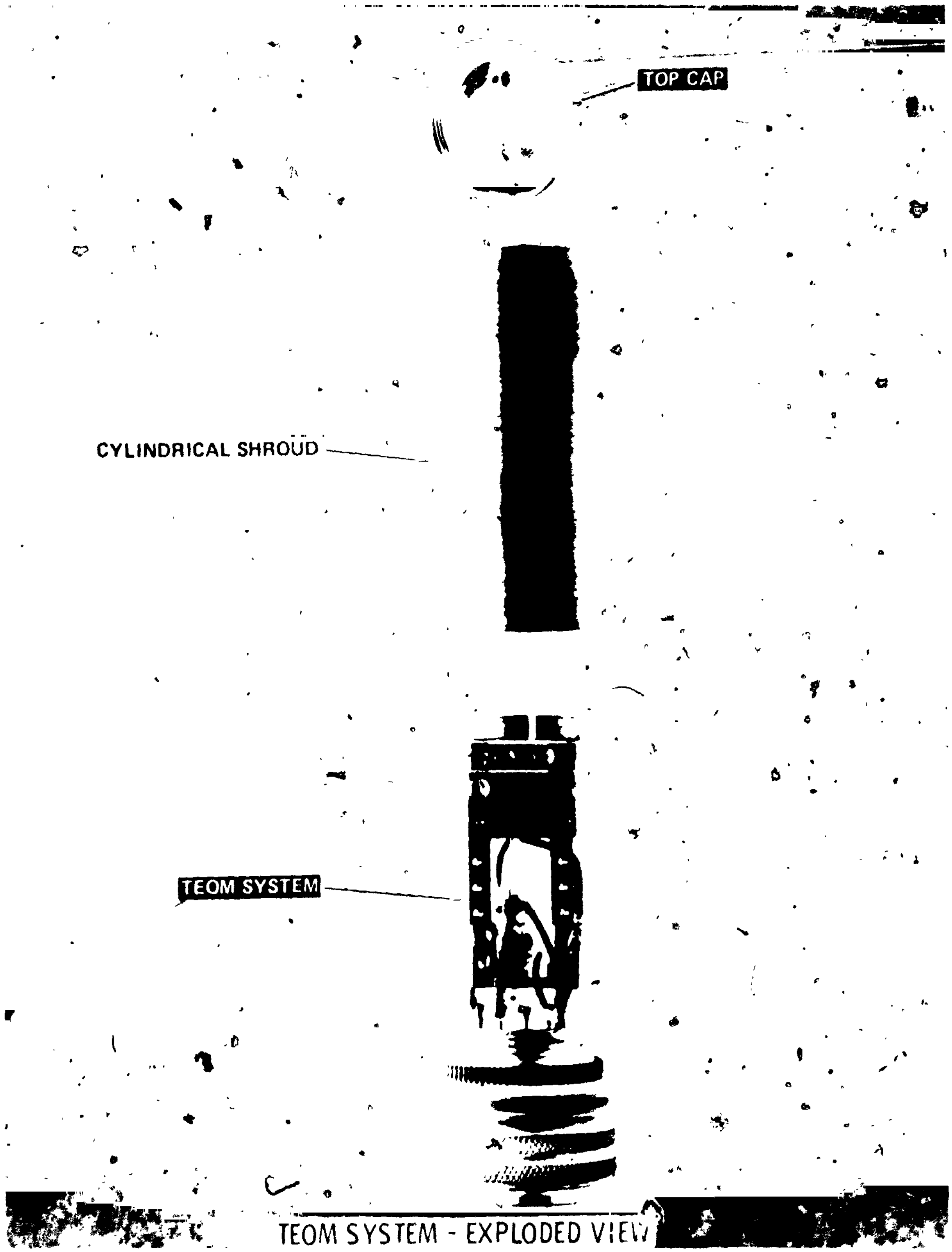

TOP CAP
CYLINDRICAL SHROUD
TEOM SYSTEM
TEOM SYSTEM - EXPLODED VIEW

Figure 27

FOLDOUT FRAME

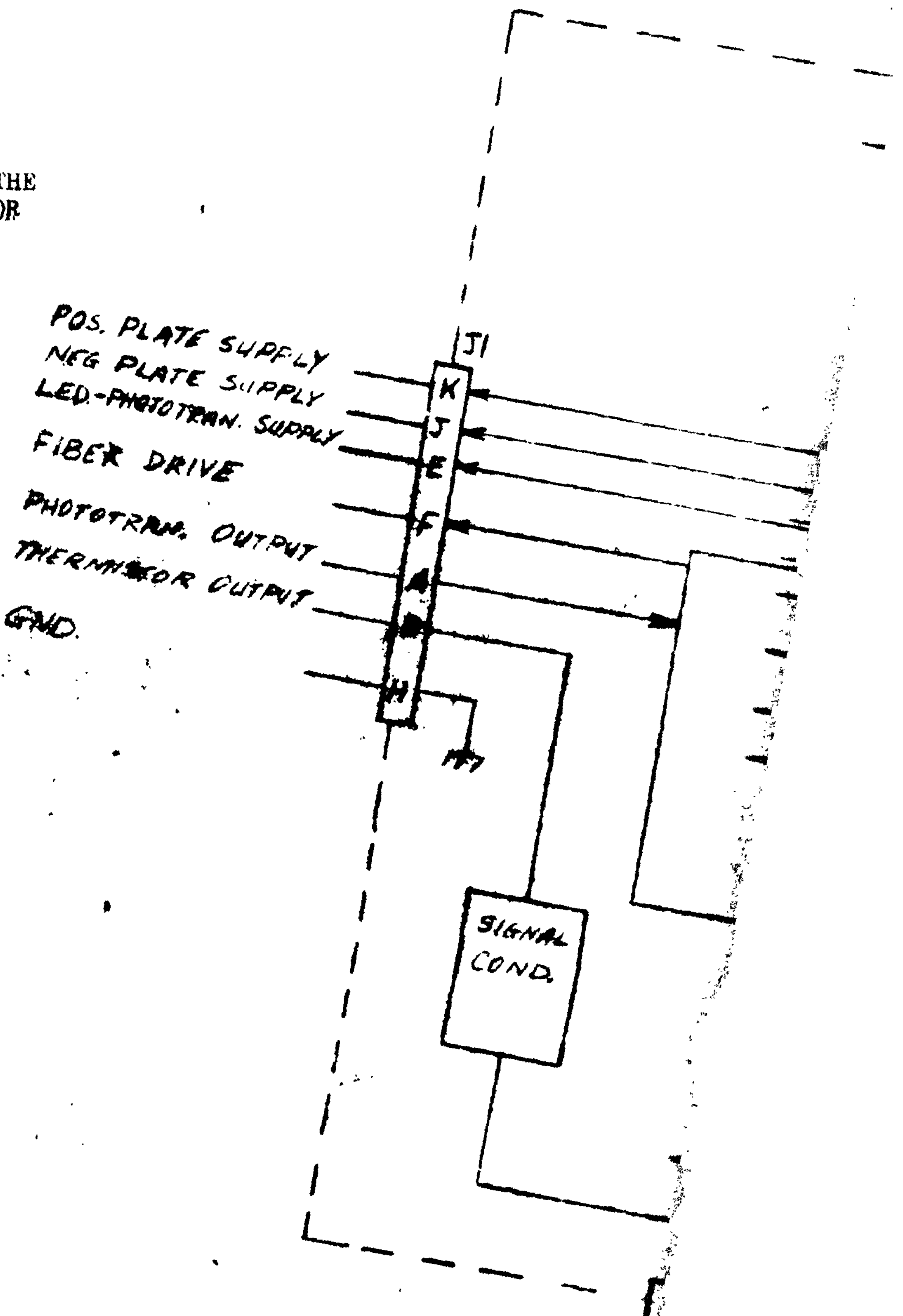

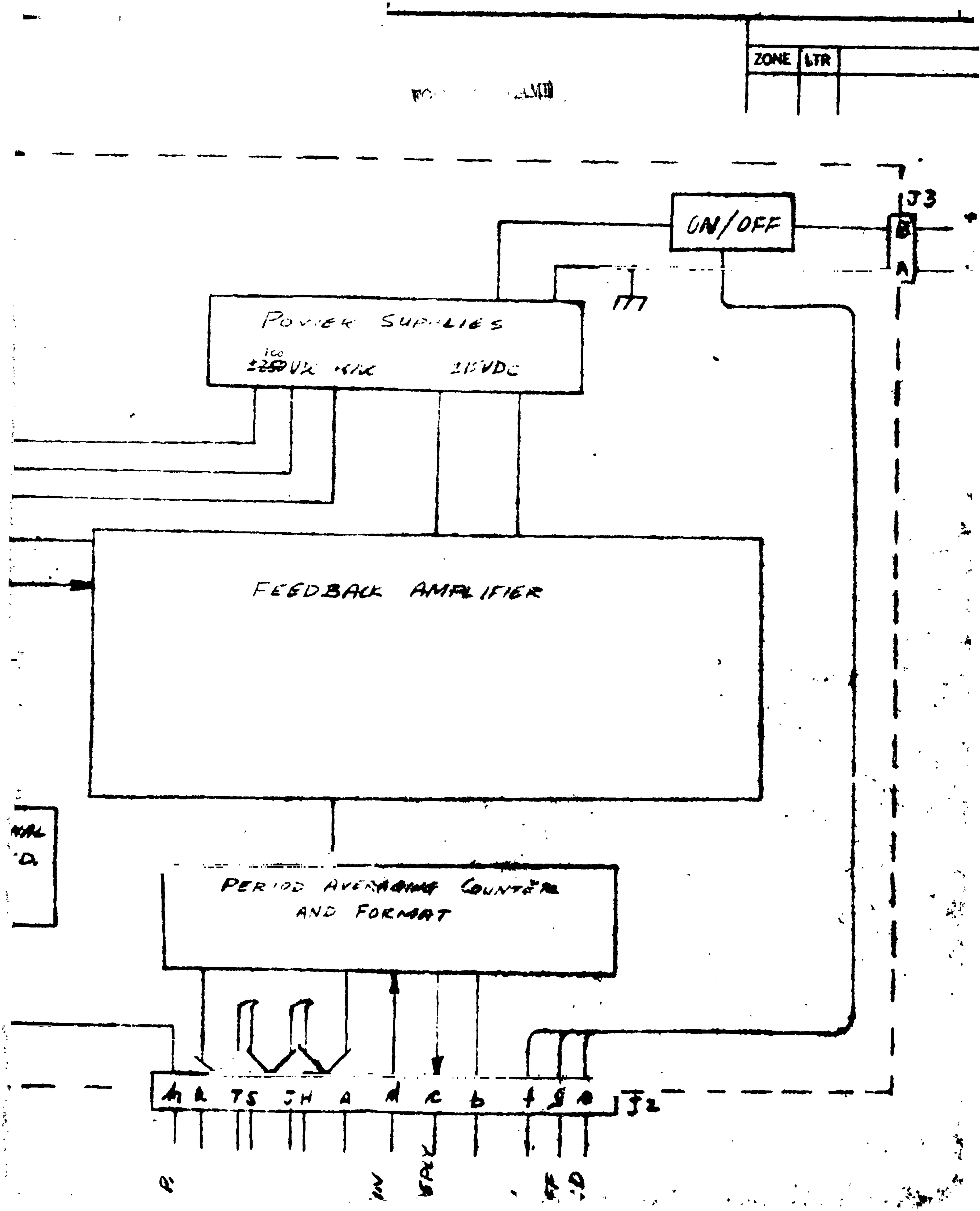

ZONE
LTR
ON/OFF
J3
B
A
POWER SUPPLIES
FEEDBACK AMPLIFIER
PERIOD AVERAGING COUNTER
AND FORMAT
J2

REVISIONS

ZONE	LTR	DESCRIPTION	DATE	APPROVED

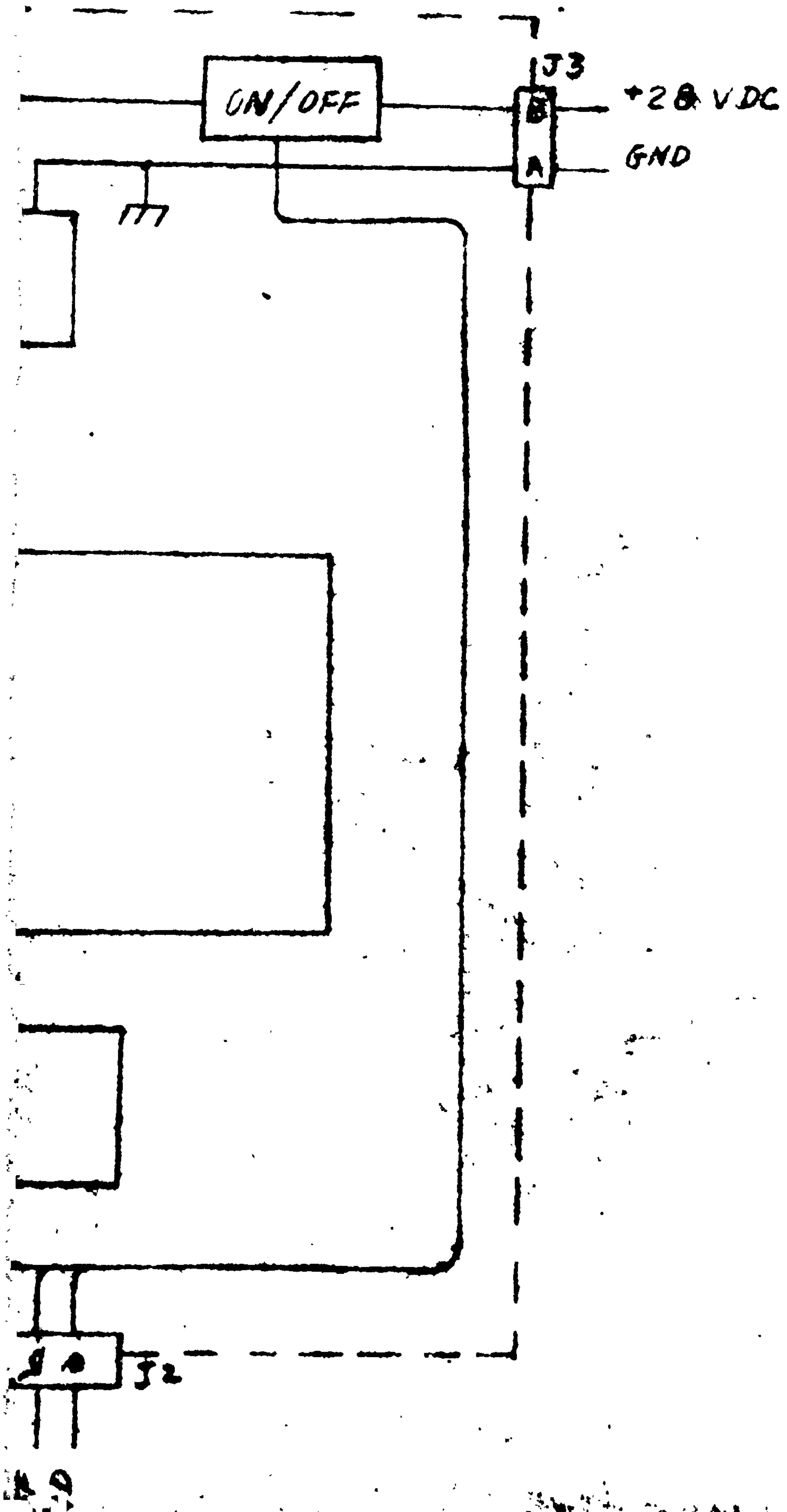

D

C

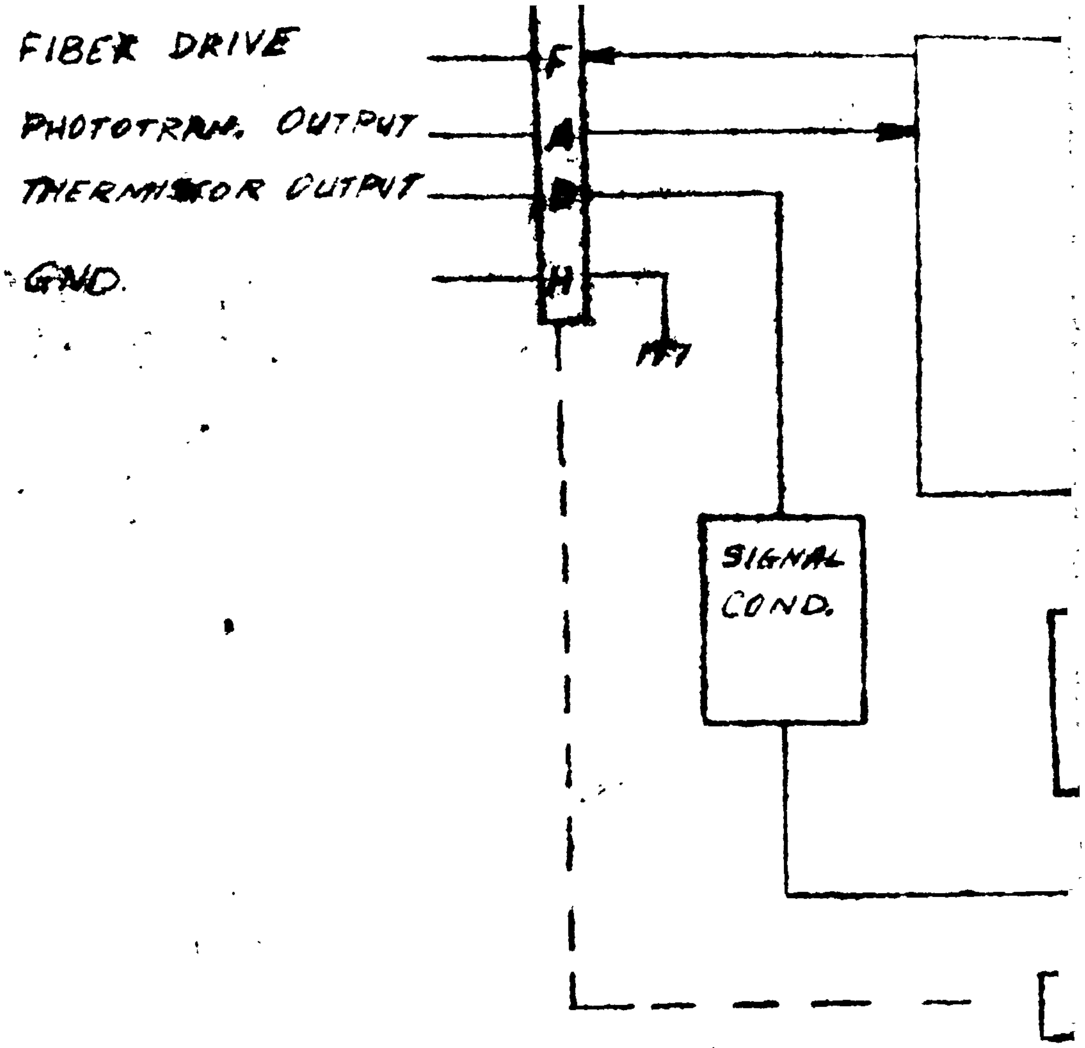
FIBER DRIVE
PHOTOTRAN. OUTPUT
THERMISTOR OUTPUT
GND.
F
A
B
H
SIGNAL COND.

NEXT ASSY

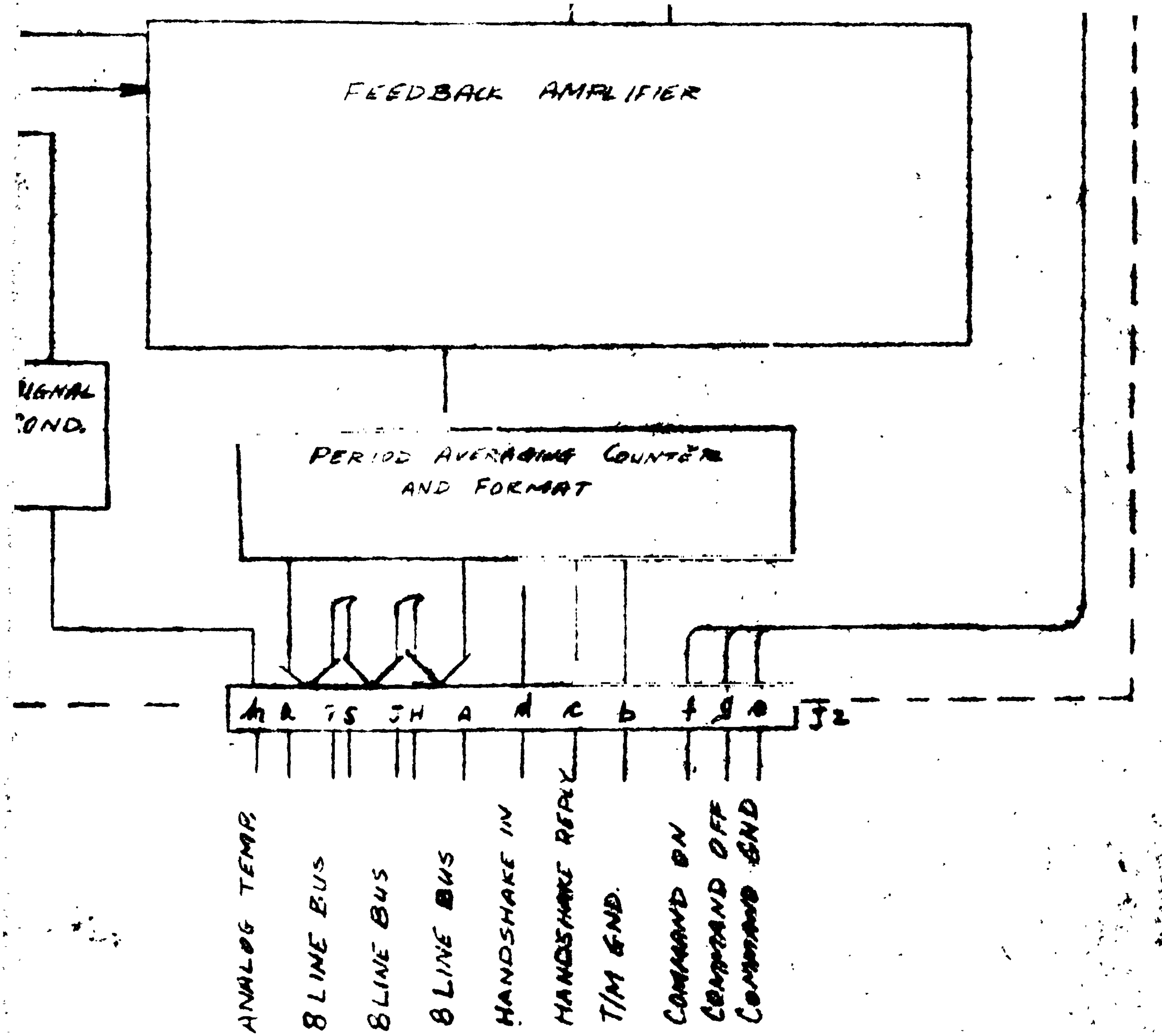

FOLDOUT FRAME

NEXT ASSY	USED ON

UNLESS OTHERWISE SPECIFIED DIMENSIONS ARE IN INCHES TOLERANCES ON

FRACTIONS ± ANGLES ±

DECIMALS .XX ± .XXX ±

MATERIAL:

FINISH:

CONTRACT NO.

DRAWN

CHECKED 7/16/72

APPD

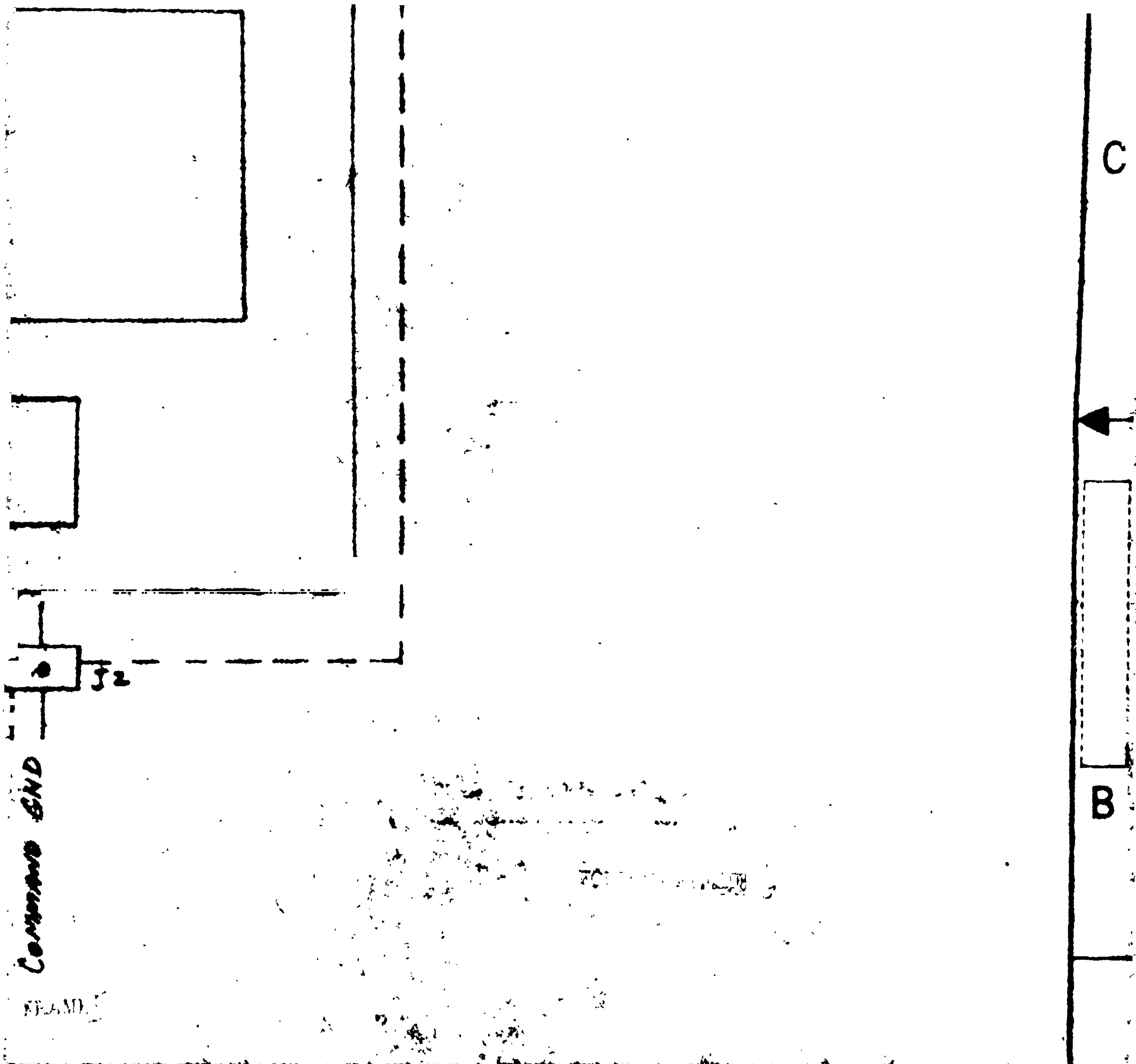

CONTRACT NO.		TEMPO INSTRUMENT PLAINVIEW, N.Y. 11803
DRAWN		TEDM ELEC. INTERFACE
CHECKED	7/6/7[illegible]	
APPD		
SIZE C	CODE IDENT NO. 07091	S 943[illegible]

FOLDOUT FRAME

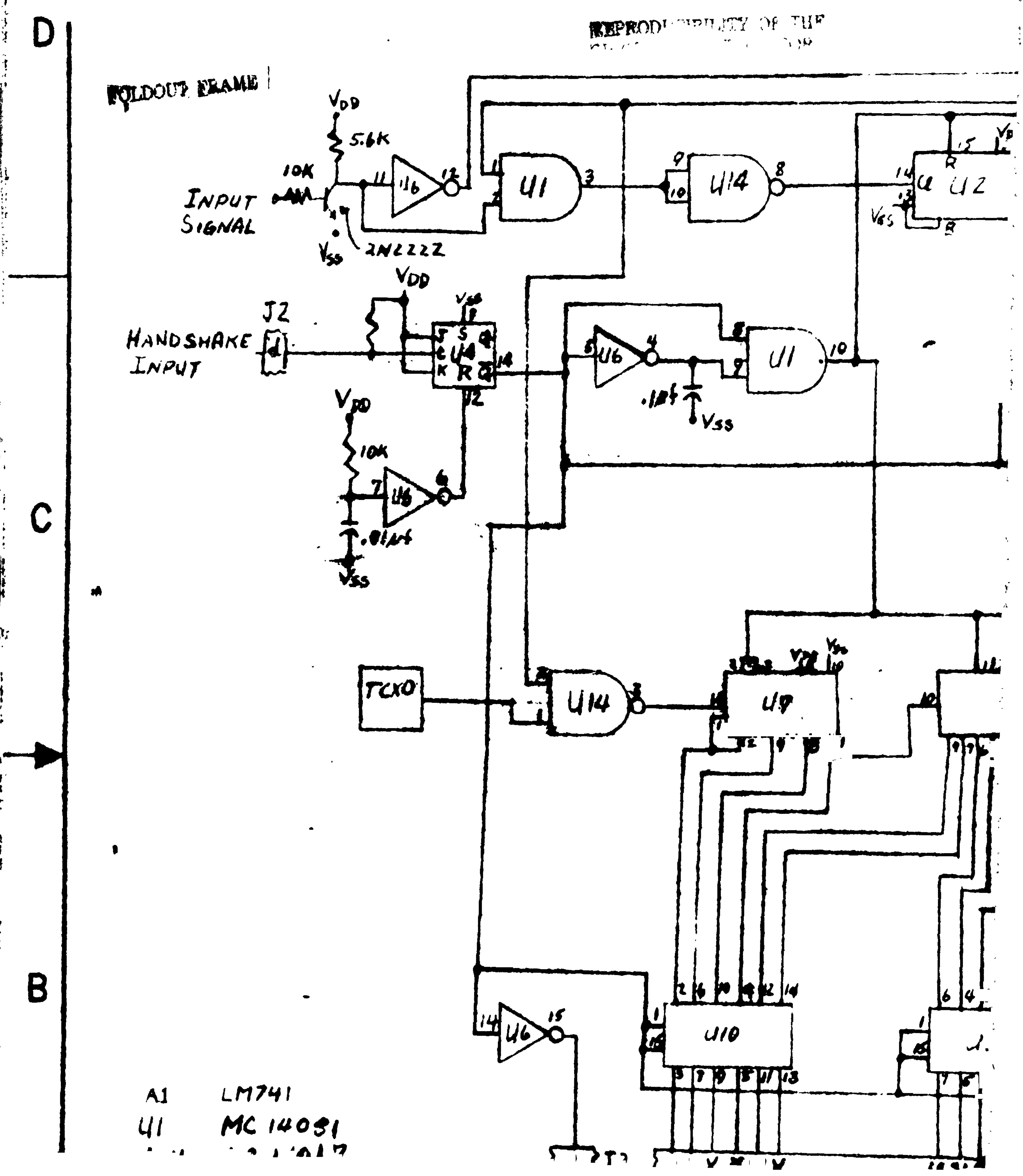

ZONE	LTR	

FOL... ...P FRAME

THE
OP

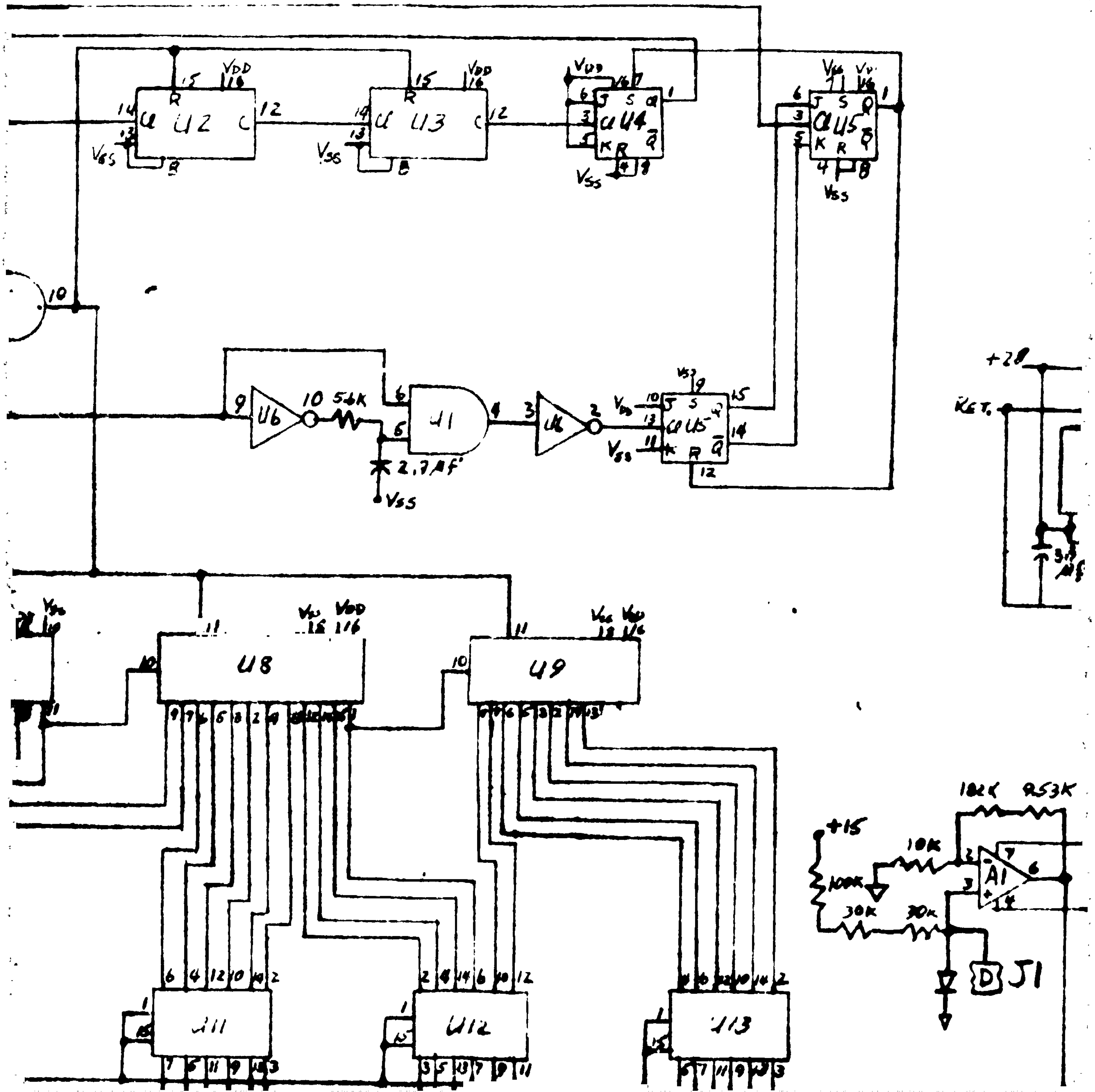

REVISIONS

ZONE	LTR	DESCRIPTION	DATE	APPROVED

D

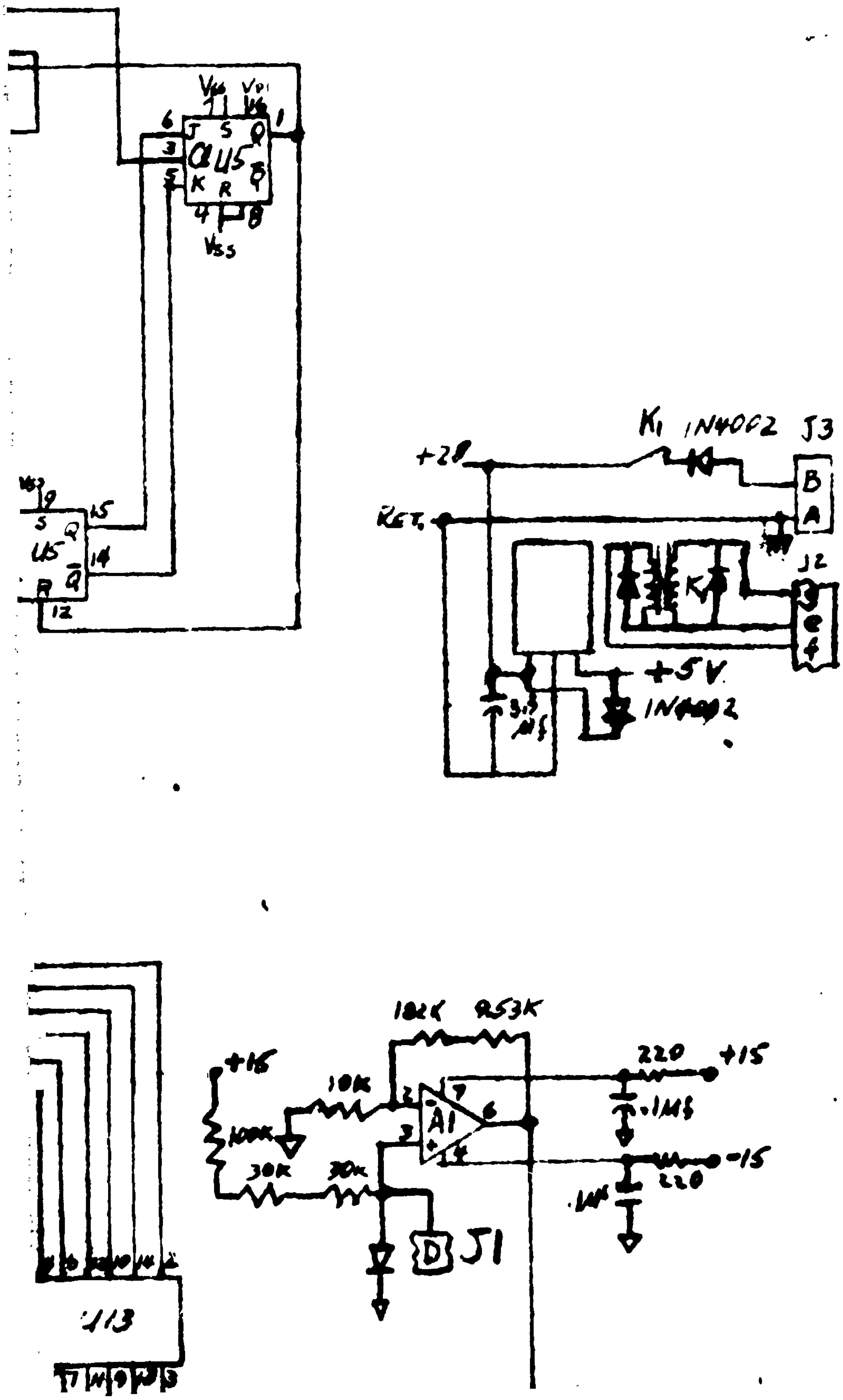

C

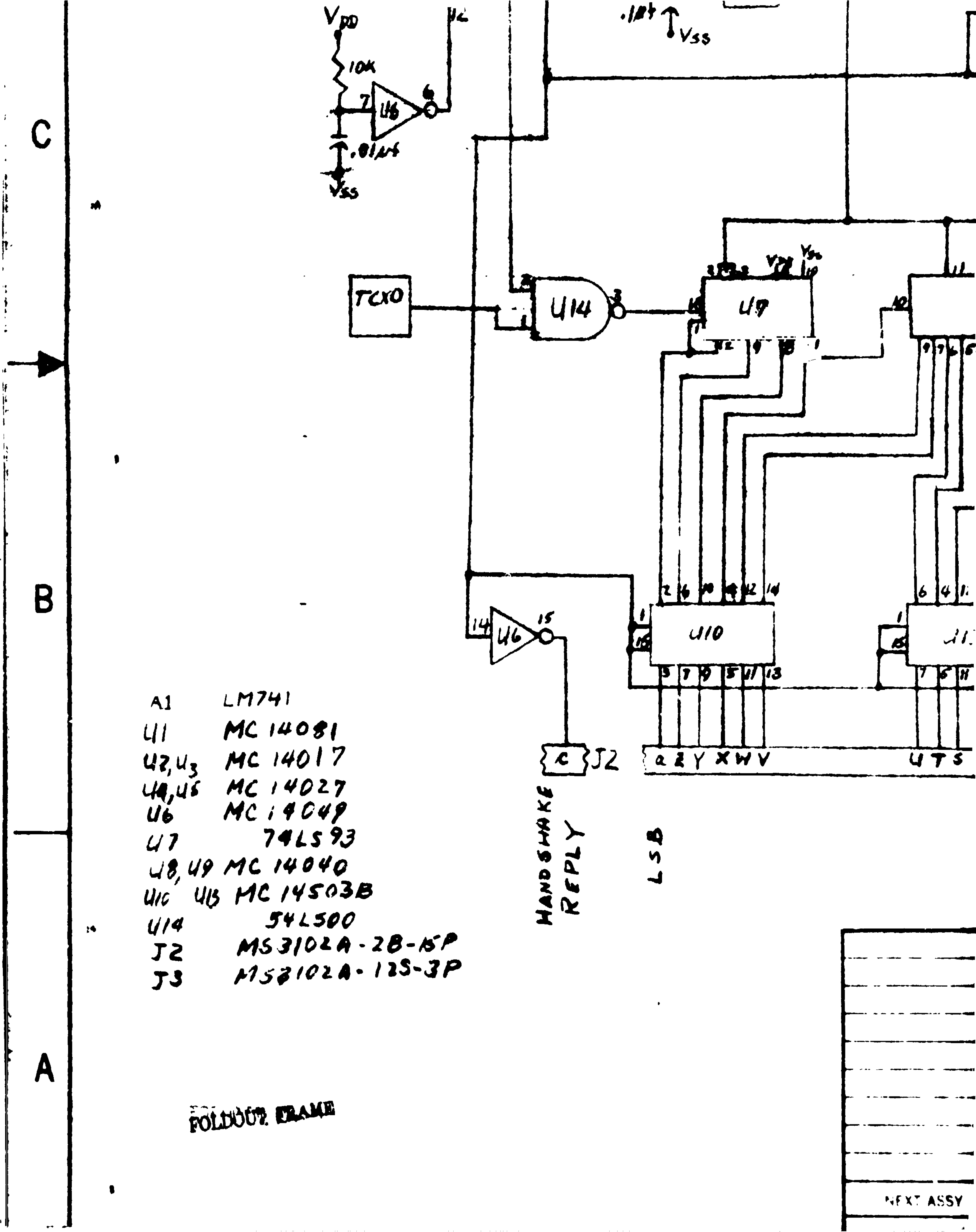

A1	LM741
U1	MC 14081
U2, U3	MC 14017
U4, U5	MC 14027
U6	MC 14049
U7	74LS93
U8, U9	MC 14040
U10 U13	MC 14503B
U14	54LS00
J2	MS3102A-28-15P
J3	MS3102A-12S-3P

FOLDOUT FRAME

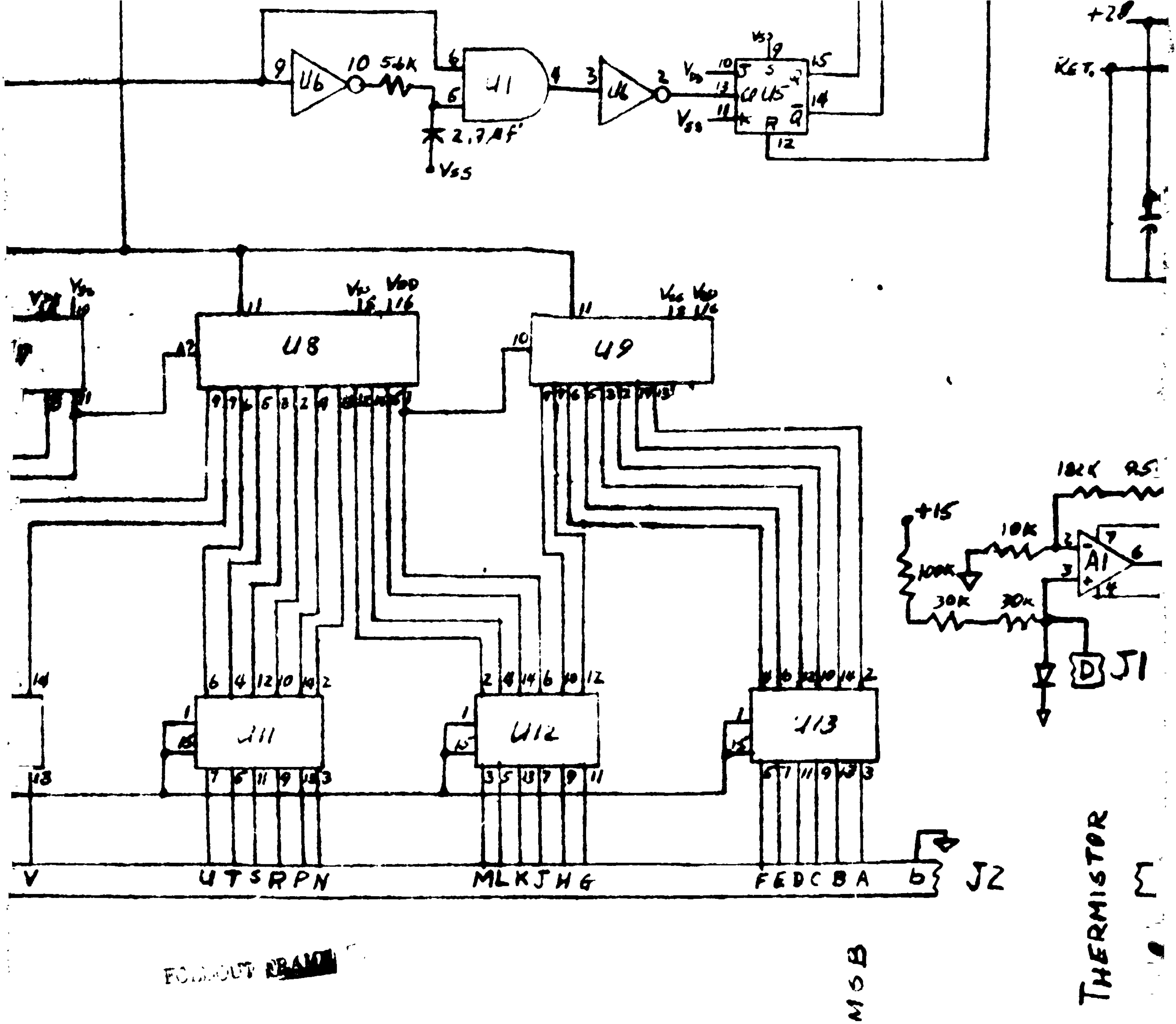

FOLDOUT FRAME

NEXT ASSY	USED ON
APPLICATION	

UNLESS OTHERWISE SPECIFIED
DIMENSIONS ARE IN INCHES
TOLERANCES ON

FRACTIONS · ANGLES

DECIMALS XX · XXX ·

MATERIAL

FINISH

CONTRACT NO.

DRAWN	M. Gorowitz	DATE 8/3
CHECKED	[illegible]	8/30
APPD		

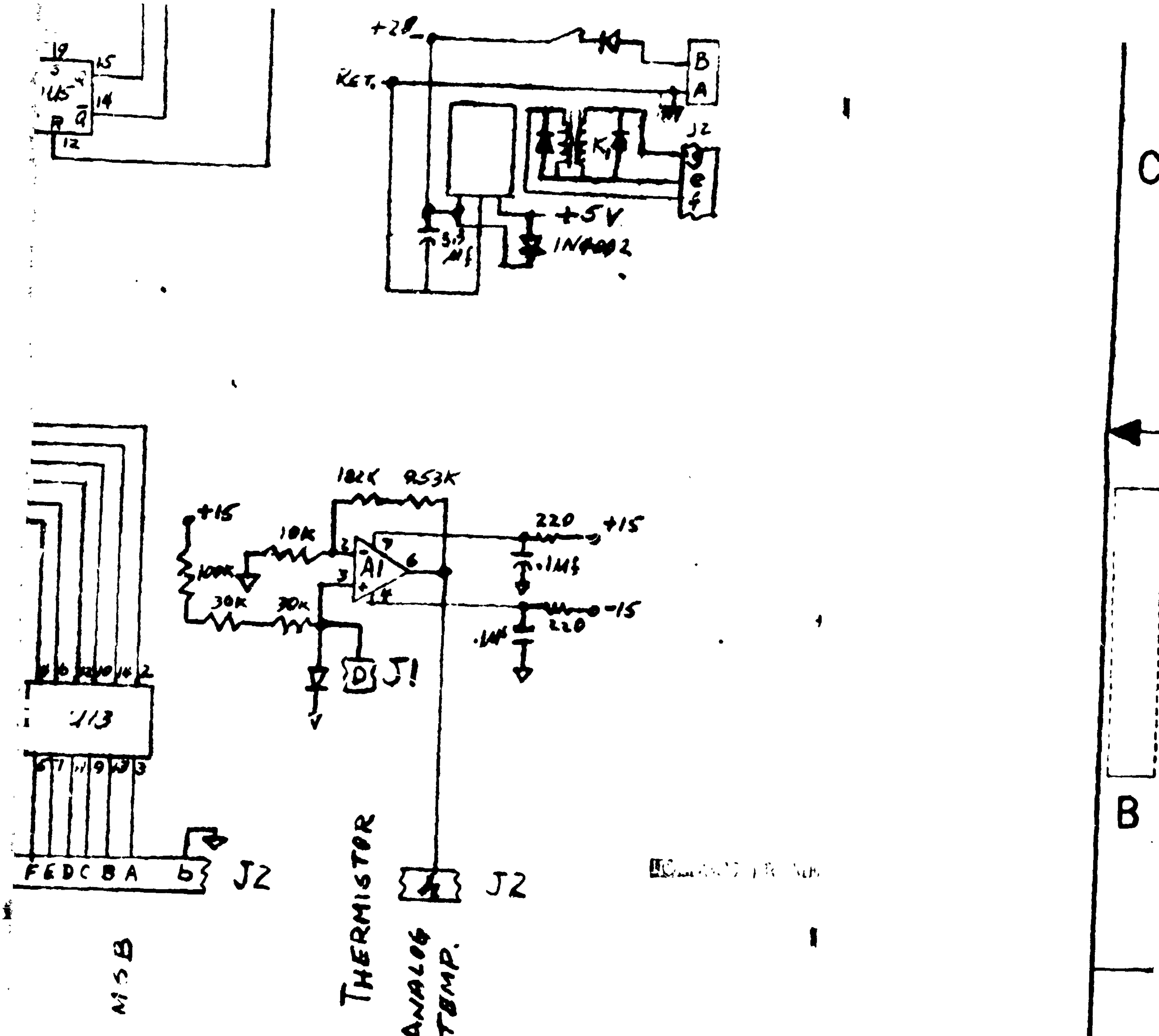

IFIED
CHES

S

CONTRACT NO.

DRAWN M. Gerkowitz | DATE 8/28/72

CHECKED | 8/30/72

APPD

TEMPO INSTRUMENT
PLAINVIEW N.Y. 11803

TECM

ELEC. INTERFACE

A

SIZE C | CODE IDENT NO 07031 | S 94317

SCALE | WEIGHT | SHEET 2 OF 2

FOLDOUT FRAME

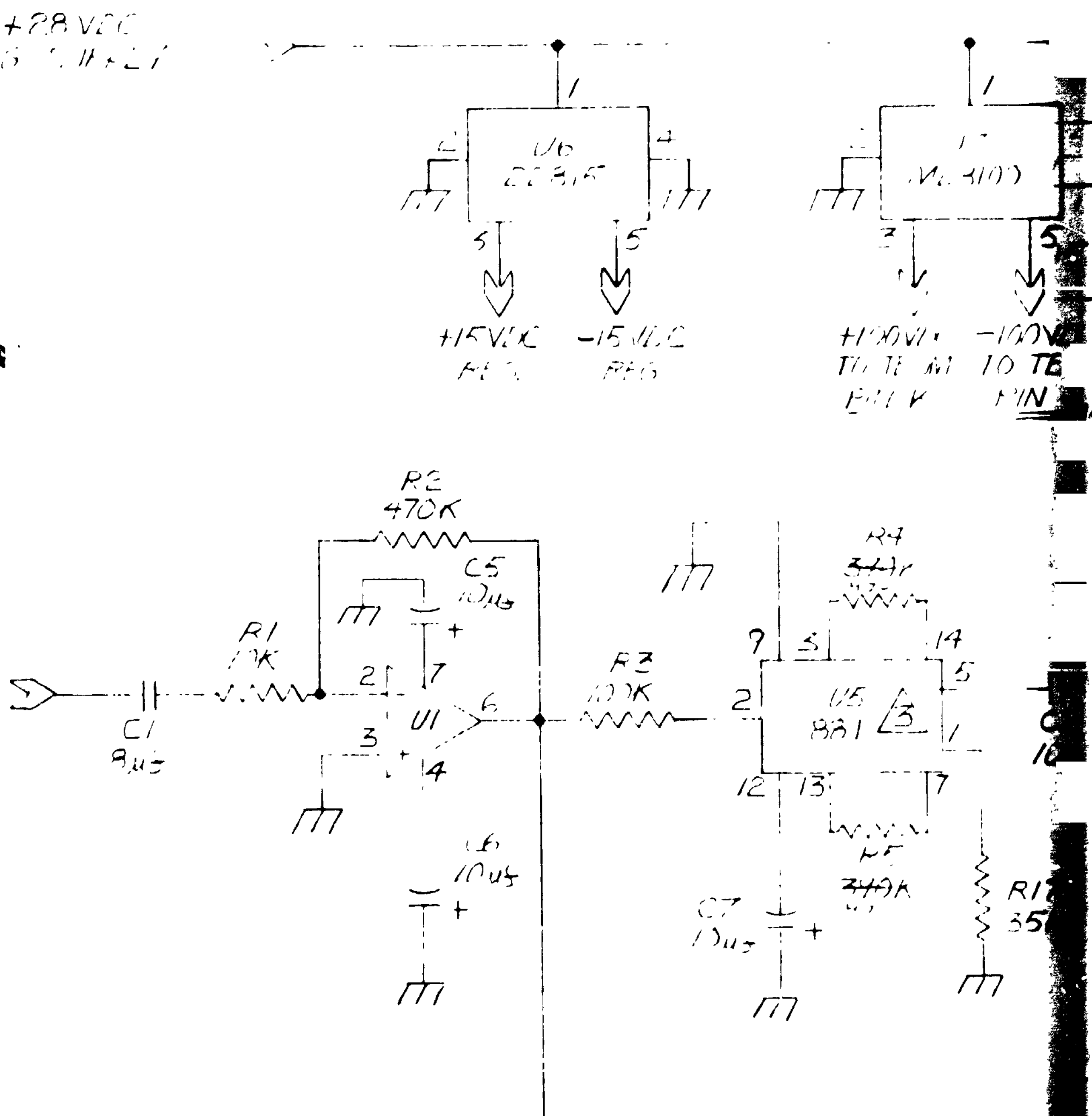

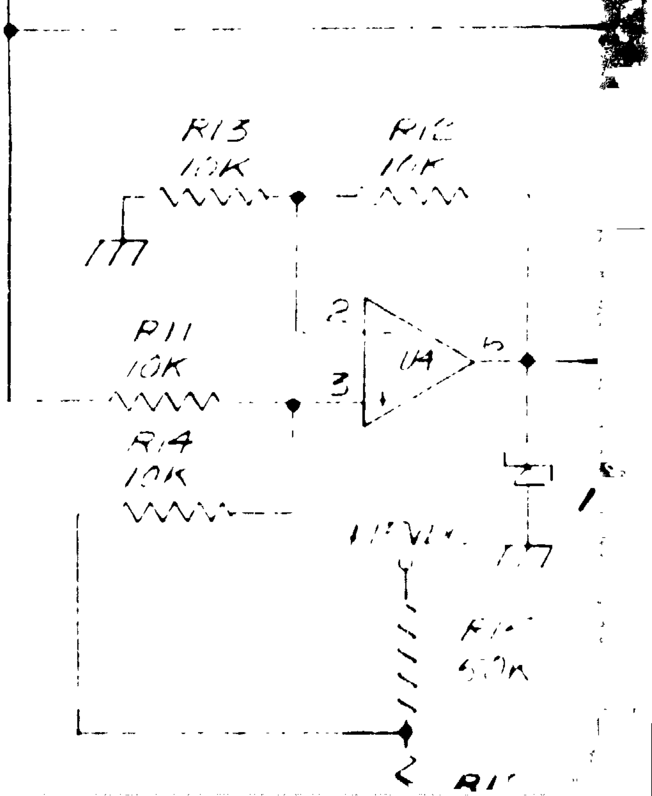

NOTES ~

1. U1, U2, U3, U4 - 741 OP AMPS.
(+15VDC, PIN 7; -15VDC, PIN 4.)
2. U5 - BECKMAN 881 ACTIVE FILTER.
(+15VDC, PIN 4; -15VDC, PIN 12)
3. BECKMAN 881 LOWPASS ROLLOFF SET BY R4, R5 (390K FOR 129 HZ.)
Q SET BY R17 (35K FOR Q = 1)
4. ALL RESISTOR VALUES IN OHMS.
5. C1, C2, C3, C4 - NON POLARIZED.
6. OPTIONAL AS REQD. FOR T/M OUTPUT
7. SIGNAL TO RACK [illegible] SINE WAVE, ZERO CROSSING, 5V + 0.5V P-P.

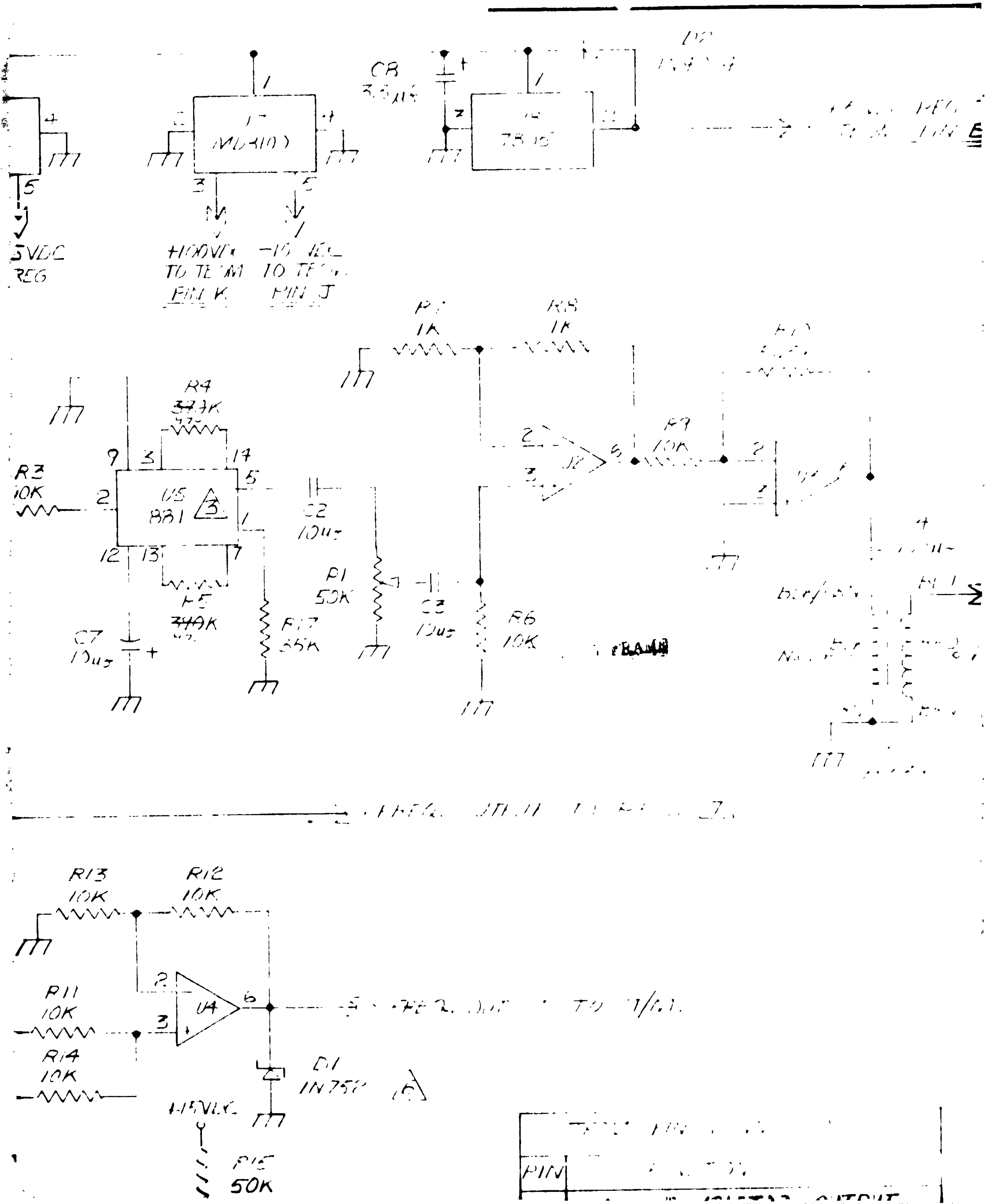
C8
MD8101
7815
5VDC
REG
TO TERM
PIN K
PIN J
R7
1K
R8
1K
R4
R3
10K
U5
881
C2
10uf
P1
50K
C3
10uf
R6
10K
R5
C7
10uf
R13
10K
R12
10K
R11
10K
R14
10K
U4
D1
IN752
50K
PIN

DATE	SYM	REVISION RECORD	AUTH	DR	CK

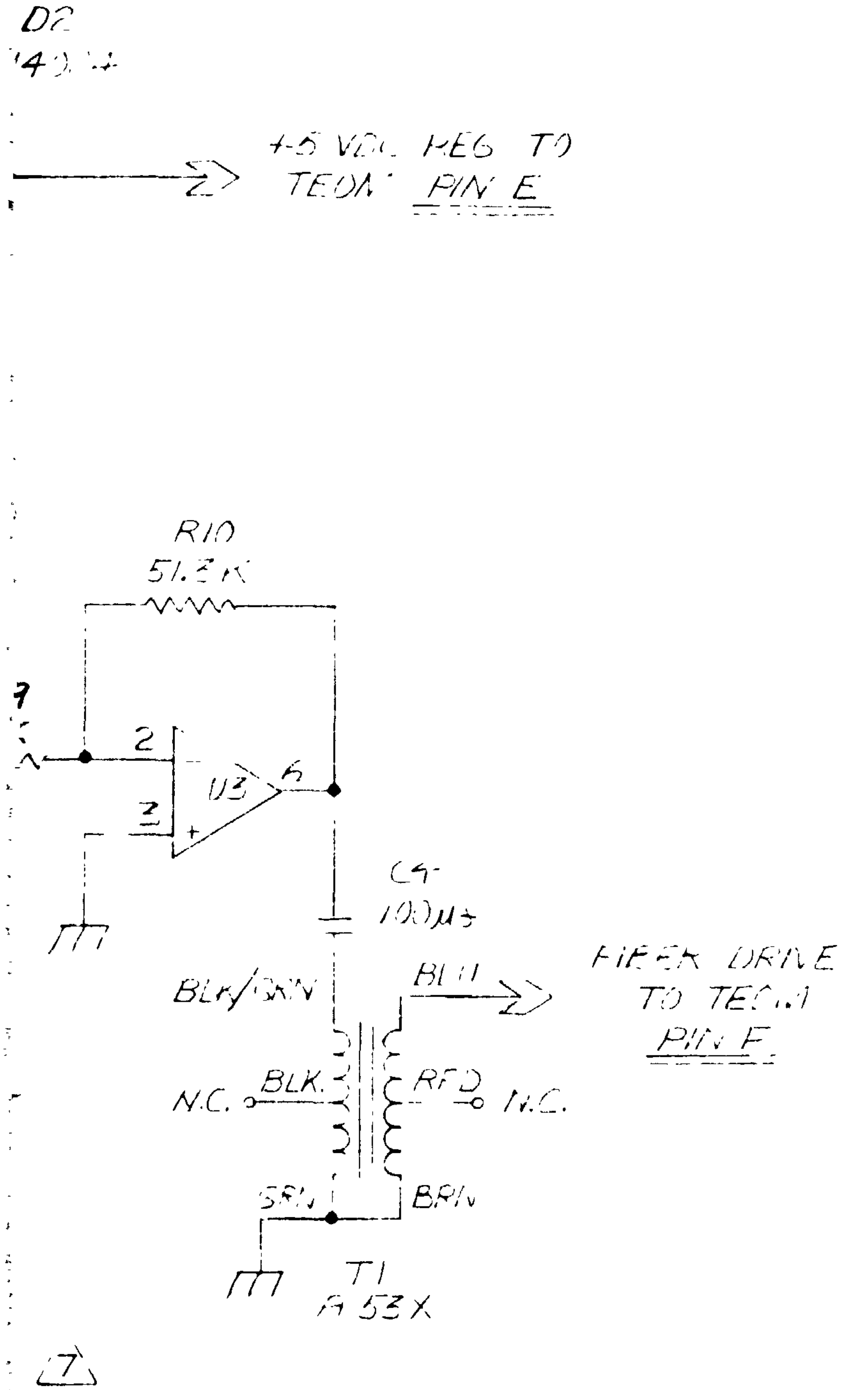

TION

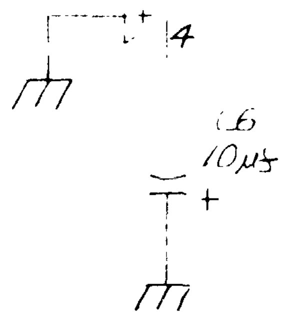

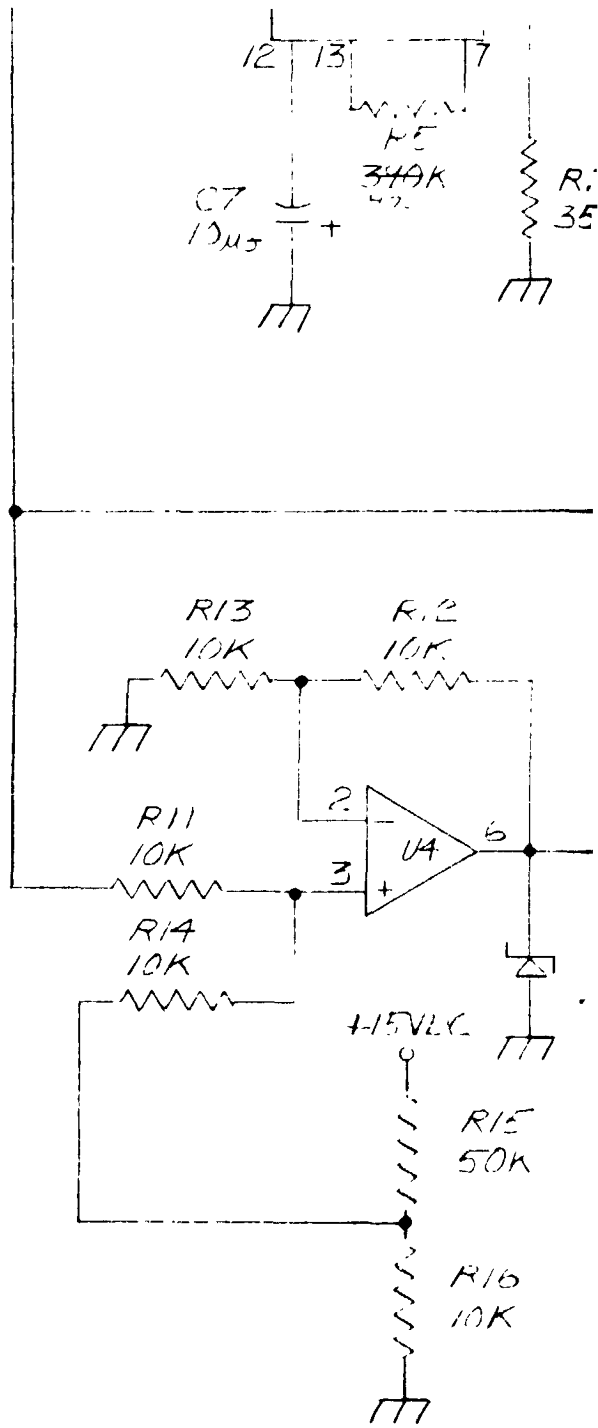

NOTES ~

1. U1, U2, U3, U4 - 741 OP AMPS.
   (+15VDC, PIN 7; -15VDC, PIN 4.)
2. U5 - BECKMAN 881 ACTIVE FILTER.
   (+15VDC, PIN 4; -15 VDC, PIN 12.)
3. (△) BECKMAN 881 LOW-PASS ROLLOFF SET BY R4, R5 (390K FOR 129 HZ.)
   Q SET BY R17 (35K FOR Q = 1)
4. ALL RESISTOR VALUES IN OHMS.
5. C1, C2, C3, C4 - NON POLARIZED.
6. (△) OPTIONAL AS REQ'D. FOR T/M OUTPUT.
7. (△) SIGNAL TO P.A.C.: NOM. 100 HZ SINE WAVE, ZERO CROSSING, 5V±0.5V P-P.

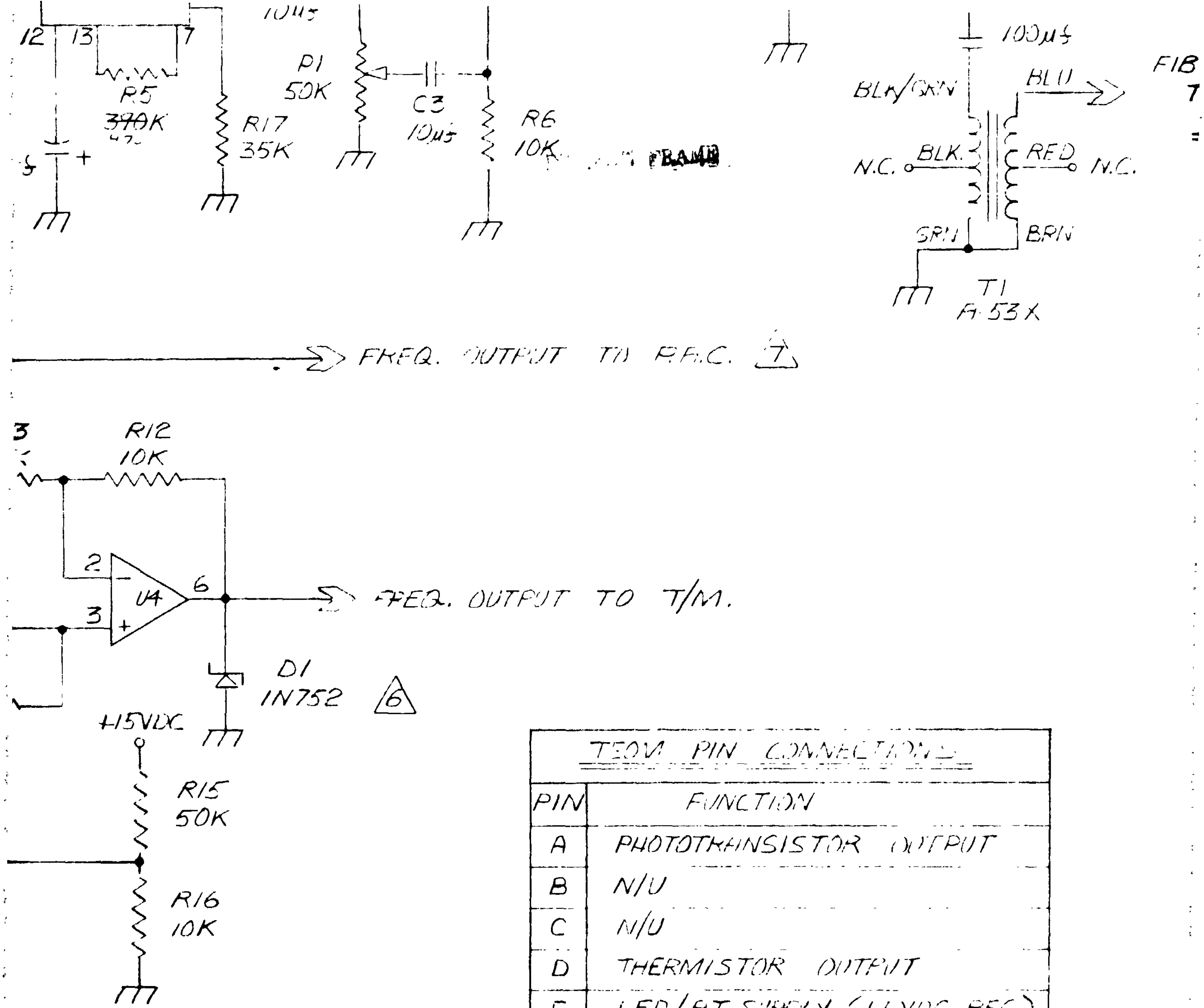

TEOM PIN CONNECTIONS

PIN	FUNCTION
A	PHOTOTRANSISTOR OUTPUT
B	N/U
C	N/U
D	THERMISTOR OUTPUT
E	LED/P.T. SUPPLY (+5VDC REG.)
F	FIBER DRIVE
G	N/U
H	GND.
J	NEG. PLATE SUPPLY
K	POS. PLATE SUPPLY
L	N/U
M	N/U
N	N/U
P	N/U

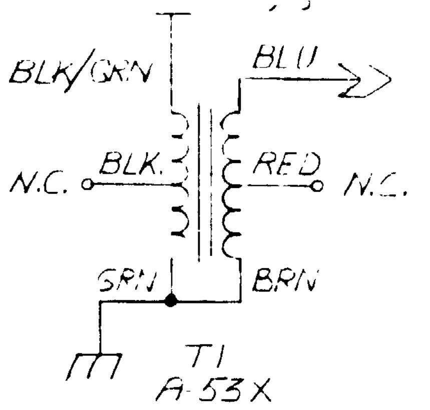

7

CONNECTIONS
TION
NSISTOR OUTPUT
OR OUTPUT
UPPLY (+5VDC REG.)
IVE
E SUPPLY
E SUPPLY

TOLERANCES (EXCEPT AS NOTED)	DUDLEY OBS.		
DECIMAL ±		SCALE	DRAWN BY / APPROVED BY
FRACTIONAL ±	TITLE FEEDBACK AMPLIFIER, SHEMATIC		
ANGULAR ±	DATE 6 JULY 1976	DRAWING NUMBER TEM-030002	

MADE IN U.S.A.